

# Probing Bound Three-Quark Excitations from Low to High Photon Virtualities

Ralf W. Gothe

UNIVERSITY OF  
SOUTH CAROLINA

NSTAR2024, June 17-21, 2024, York, England



- Why are  $\gamma_V NN^*$  electrocouplings interesting? Probing bound valence quarks, baryon wave functions, the emergence of mass, and finally strong QCD.
- What is experimentally possible? Measuring continuously the distance-dependent bound dressed quark structure of  $N^*$ 's mapping the transition to pQCD.
- What is needed beyond CLAS12? Higher beam energy, high acceptance (exclusive), and high-luminosity detector (beam time) with good  $W$  resolution.

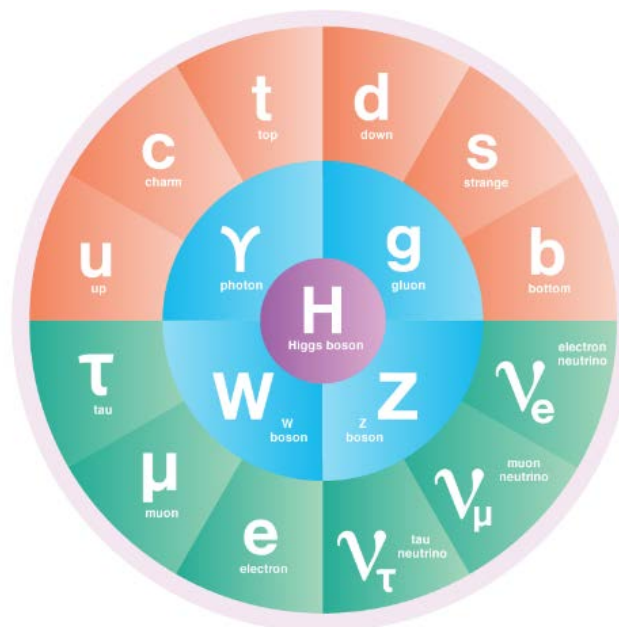
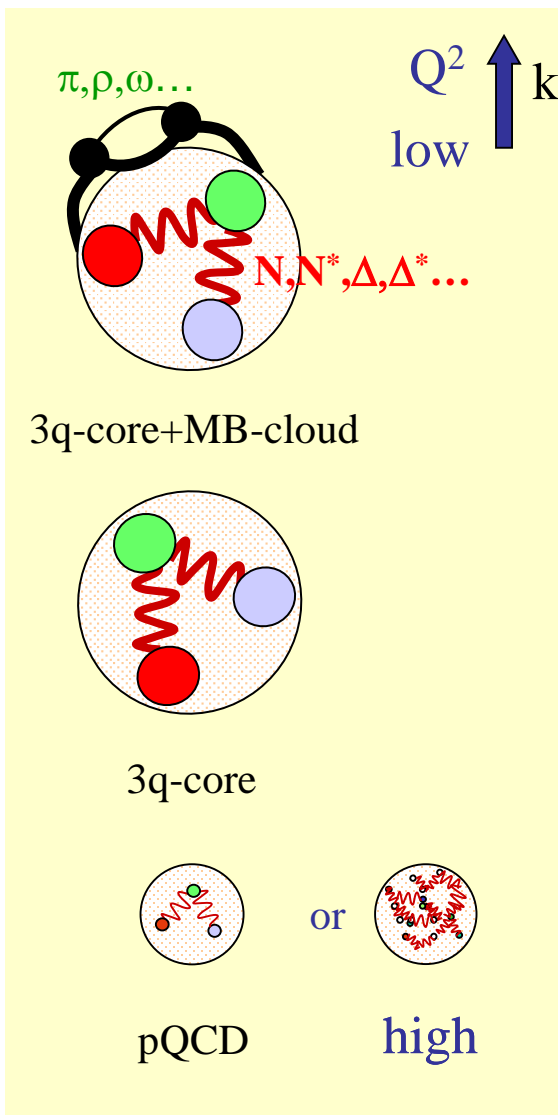
This work is supported in parts by the National Science Foundation under Grant PHY 10011349.

---

# Why is it Interesting?

# Emergence of Hadron Mass Traced by Electromagnetic Probes

# SM



● QUARKS ● LEPTONS ● BOSONS ● HIGGS BOSON

$$\mathcal{L} = \frac{1}{4g^2} G_{\mu\nu}^a G_{\mu\nu}^a + \sum_j \bar{q}_j (i \not{\partial} D_\mu + m_j) q_j$$

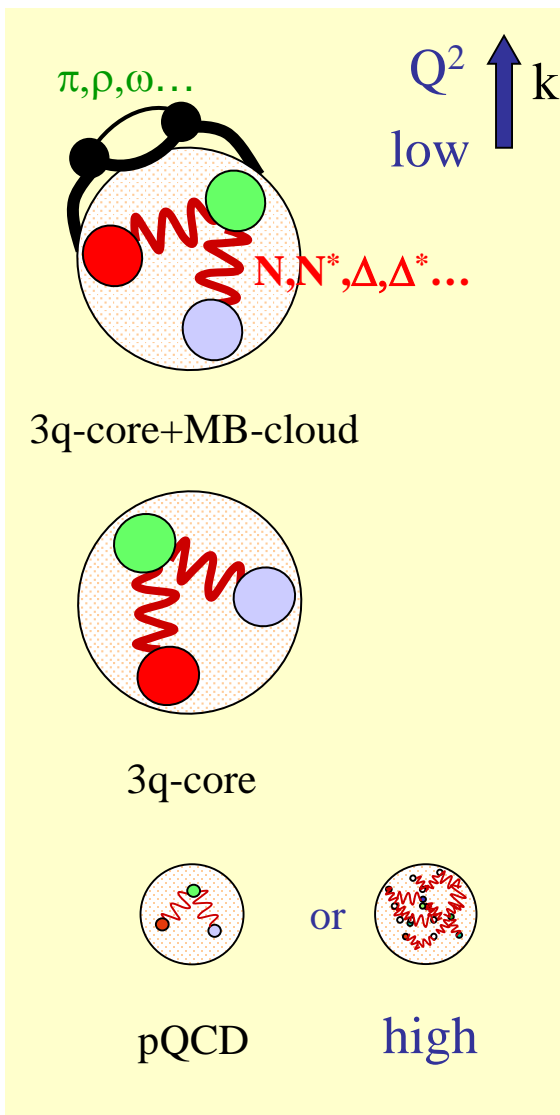
where  $G_{\mu\nu}^a \equiv \partial_\mu A_\nu^a - \partial_\nu A_\mu^a + if_{bc}^a A_\mu^b A_\nu^c$

and  $D_\mu \equiv \partial_\mu + it^a A_\mu^a$

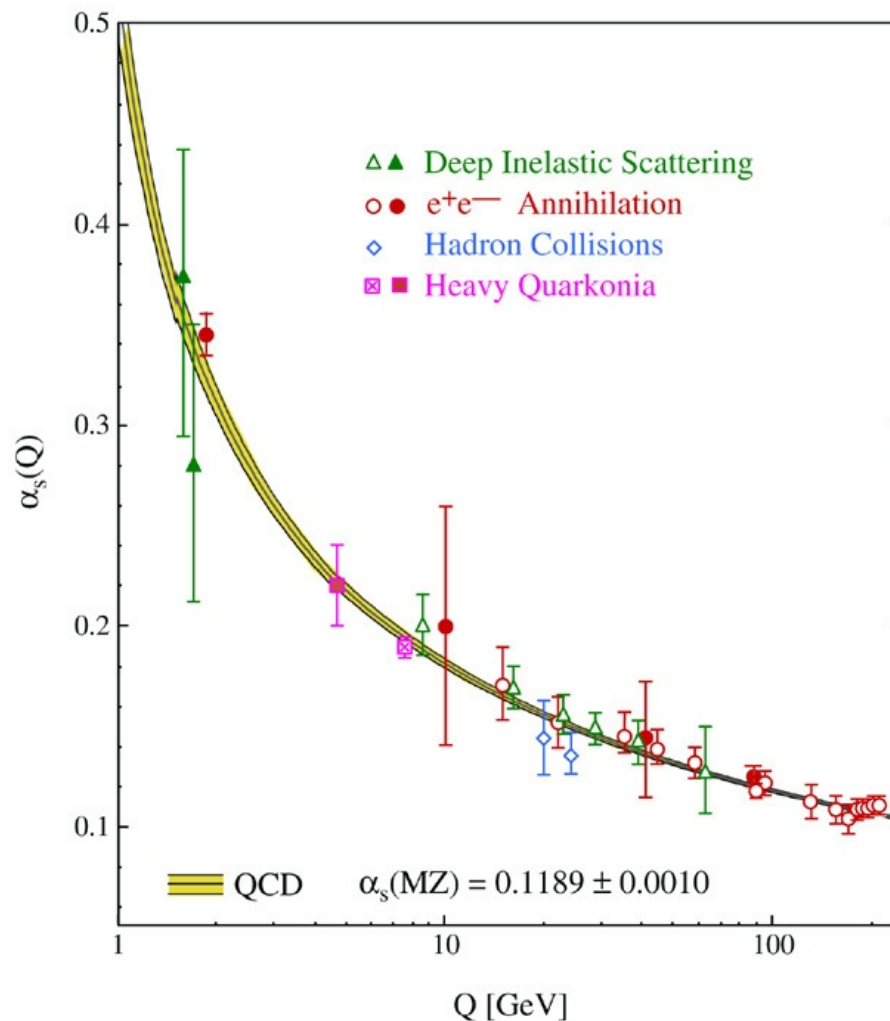
That's it!

Frank Wilczek, Physics Today, August 2000

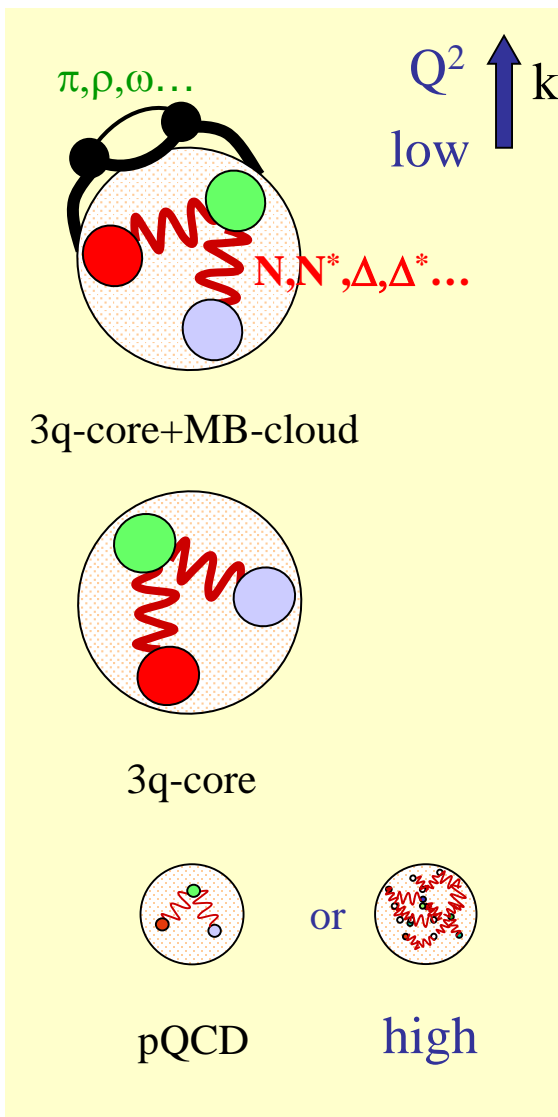
# Hadron Structure with Electromagnetic Probes



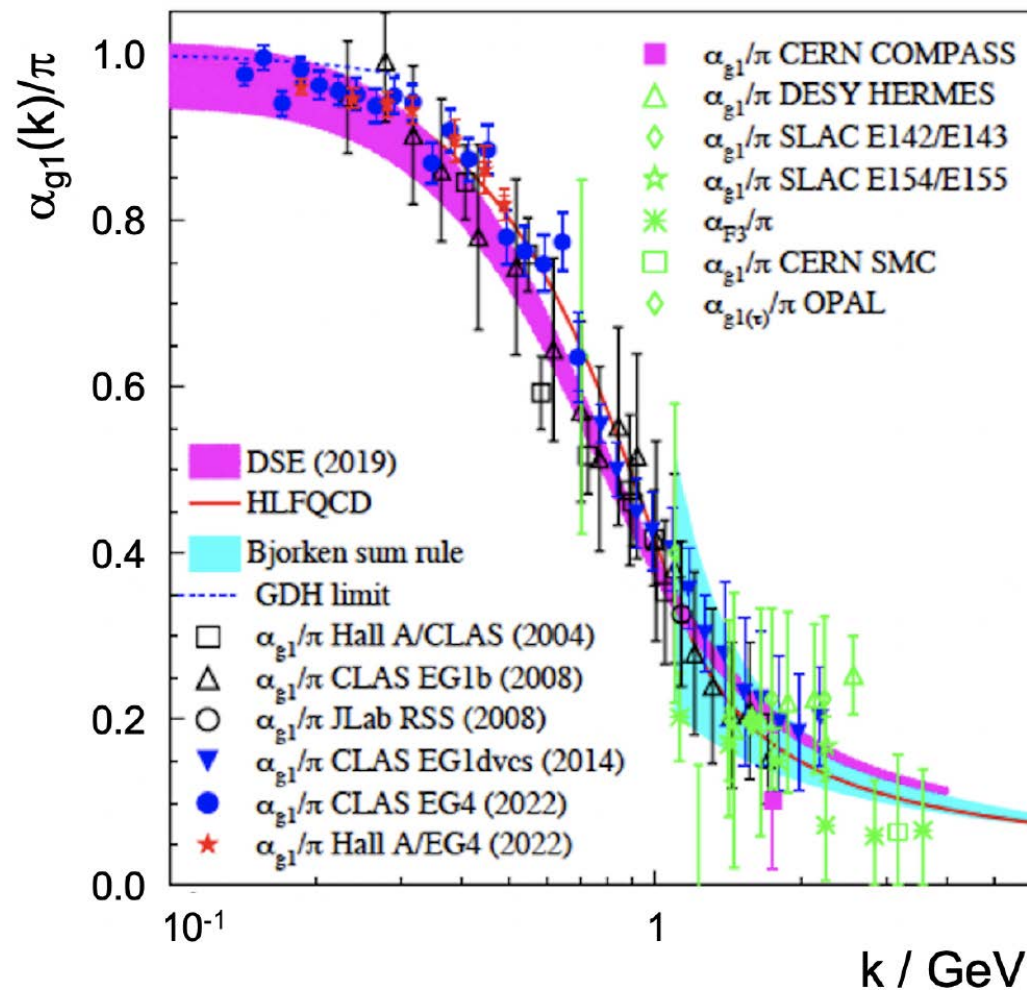
- The SM  $\alpha_s$  diverges as  $\Lambda_{\text{QCD}}^2$  approaches zero, but confinement and the meson cloud heal this artificial divergence as QCD becomes non-perturbative.



# Hadron Structure with Electromagnetic Probes



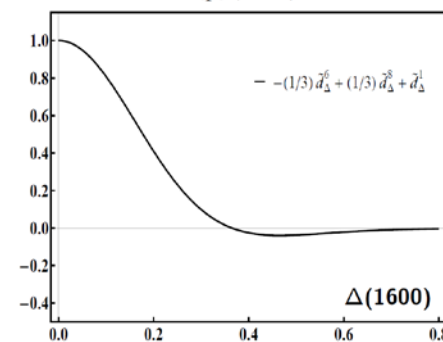
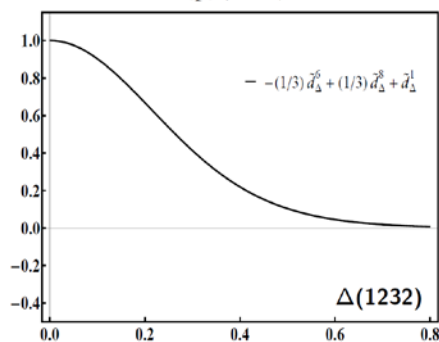
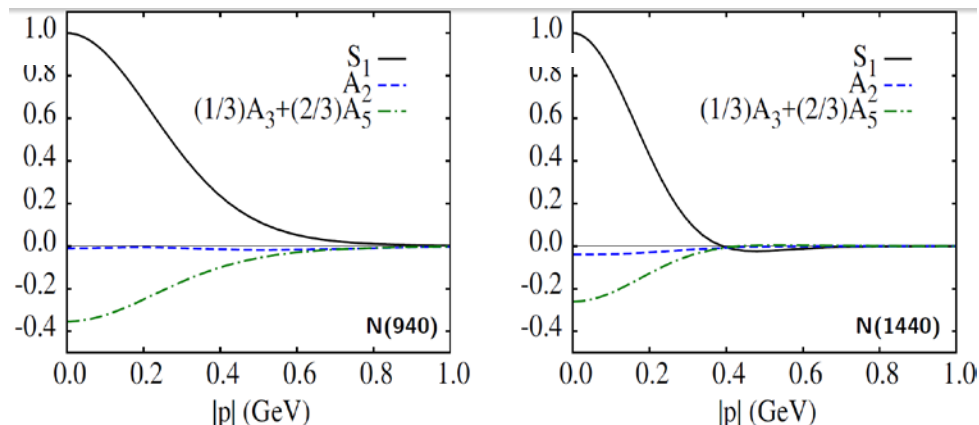
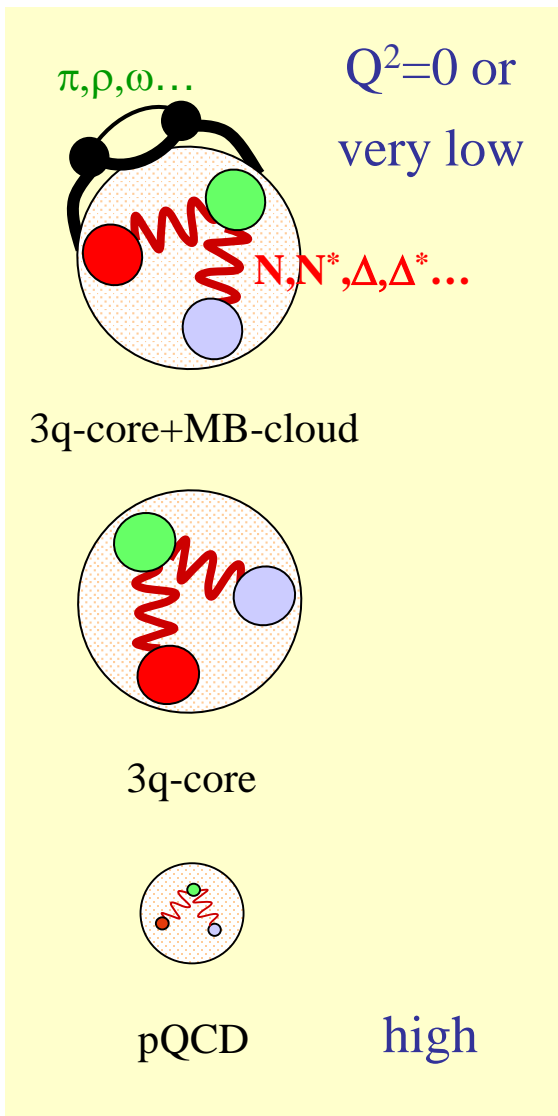
- The SM  $\alpha_s$  diverges as  $\Lambda_{\text{QCD}}^2$  approaches zero, but confinement and the meson cloud heal this artificial divergence as QCD becomes non-perturbative.





# Hadron Spectrum with Electromagnetic Probes

CSM



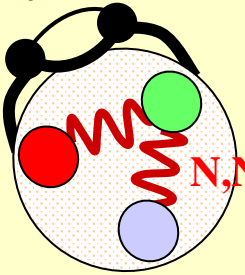
|              | $N(940)$ | $N(1440)$ | $\Delta(1232)$ | $\Delta(1600)$ |
|--------------|----------|-----------|----------------|----------------|
| scalar       | 62%      | 62%       | —              | —              |
| pseudovector | 29%      | 29%       | 100%           | 100%           |
| mixed        | 9%       | 9%        | —              | —              |
| $S$ -wave    | 0.76     | 0.85      | 0.61           | 0.30           |
| $P$ -wave    | 0.23     | 0.14      | 0.22           | 0.15           |
| $D$ -wave    | 0.01     | 0.01      | 0.17           | 0.52           |
| $F$ -wave    | —        | —         | $\sim 0$       | 0.02           |



# Hadron Spectrum with Electromagnetic Probes

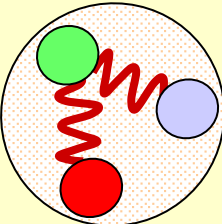
CSM

$\pi, \rho, \omega, \dots$   $Q^2=0$  or very low




$N, N^*, \Delta, \Delta^*, \dots$

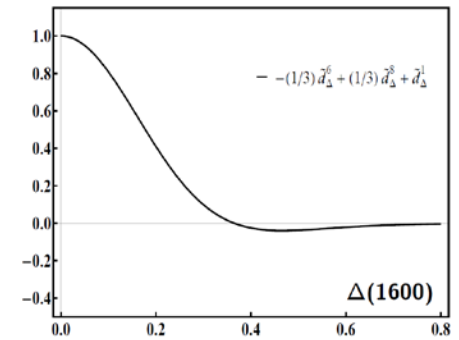
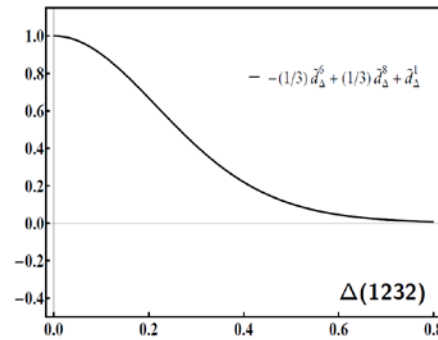
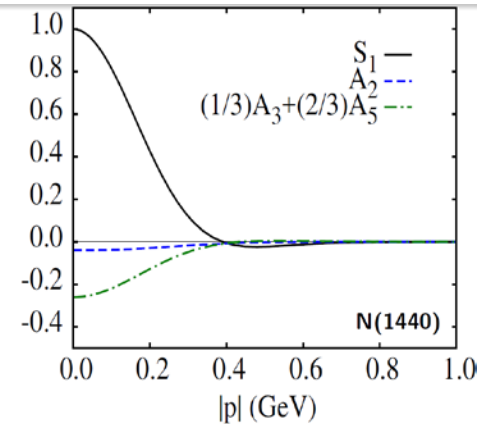
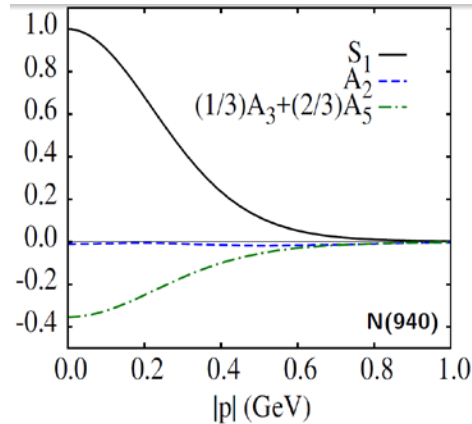
3q-core+MB-cloud




3q-core




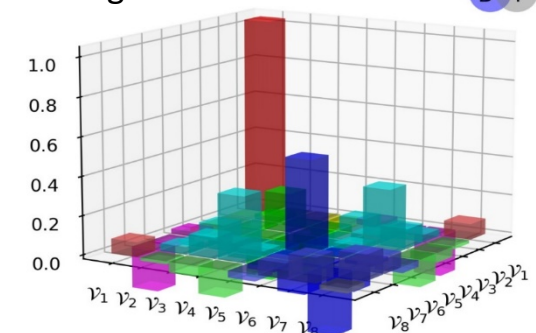
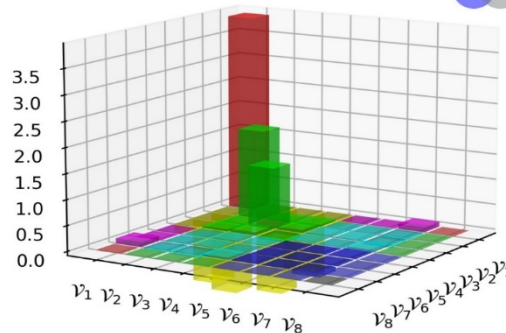
pQCD high



$\Delta(1232) \frac{3^+}{2}$  mainly  $S$ -wave.



$\Delta(1600) \frac{3^+}{2}$  mainly  $S$ -wave, but significant  $D$ -wave.

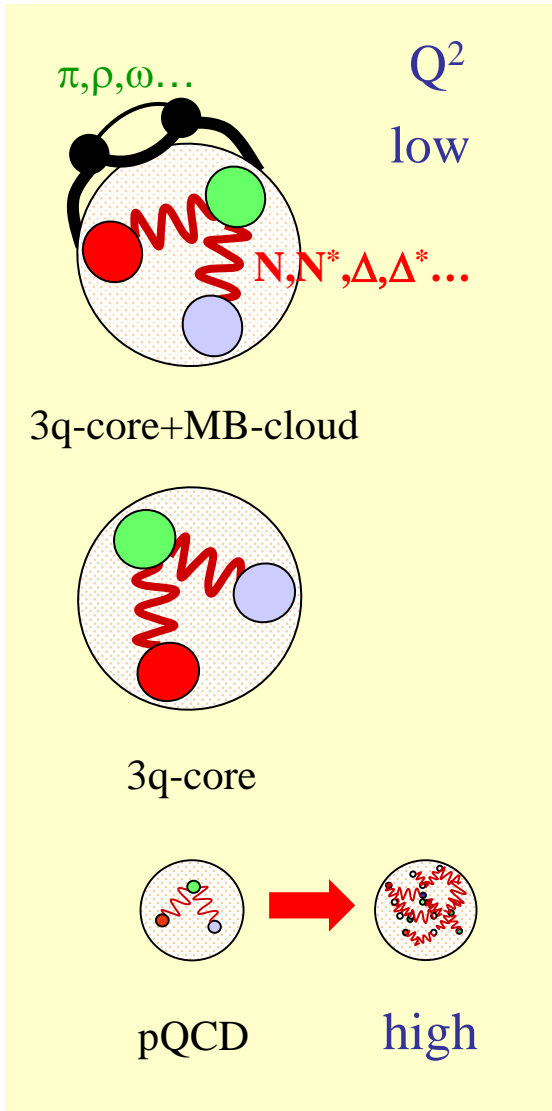





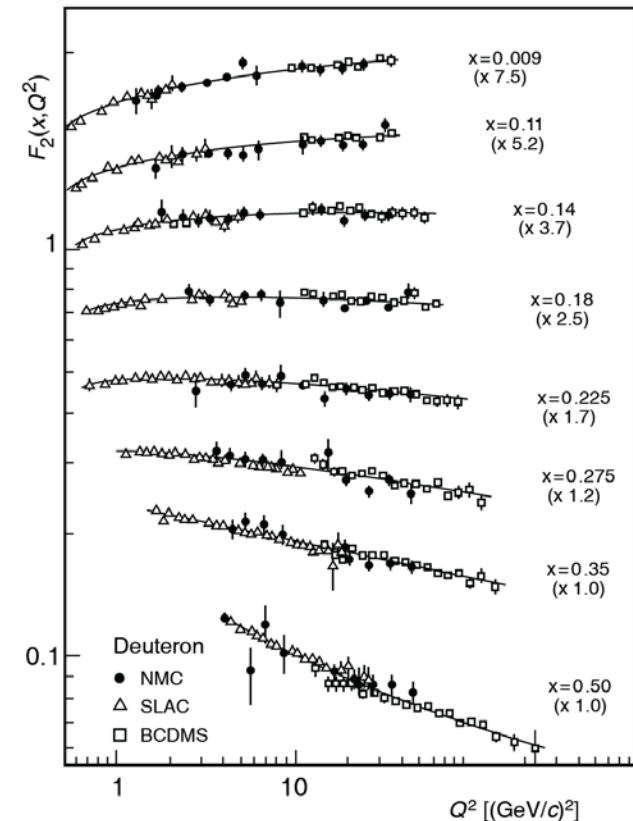
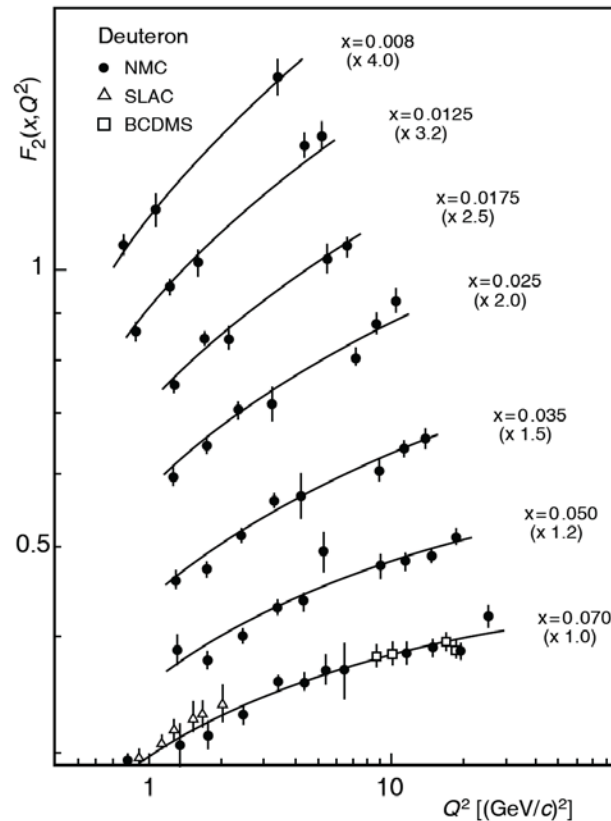
---

# Experimental Approach

# Hadron Structure and Emergence of Hadron Mass

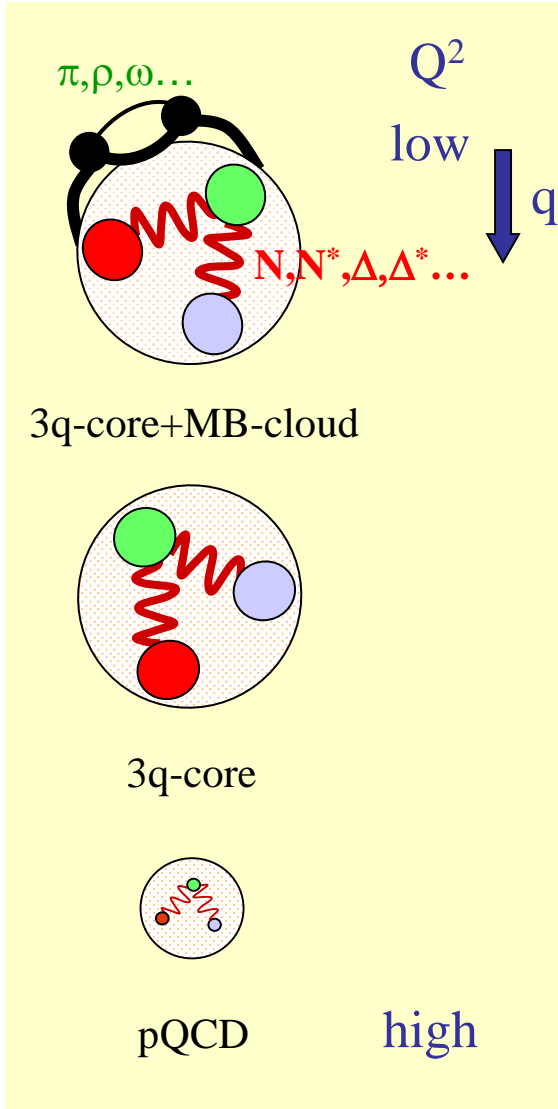


➤ Study the structure of the nucleon ground state.

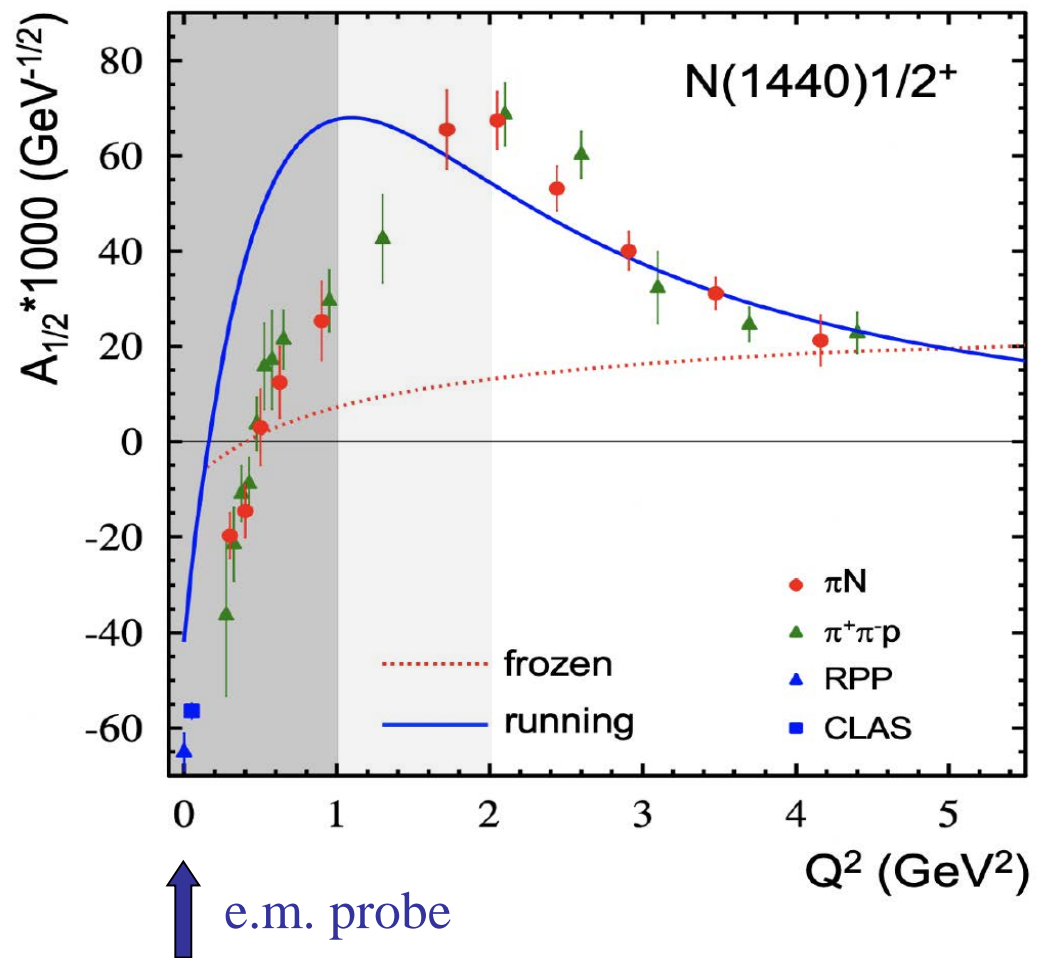


➔ 
$$F_2(x) = x \cdot \sum_f z_f^2 (q_f(x) + \bar{q}_f(x))$$

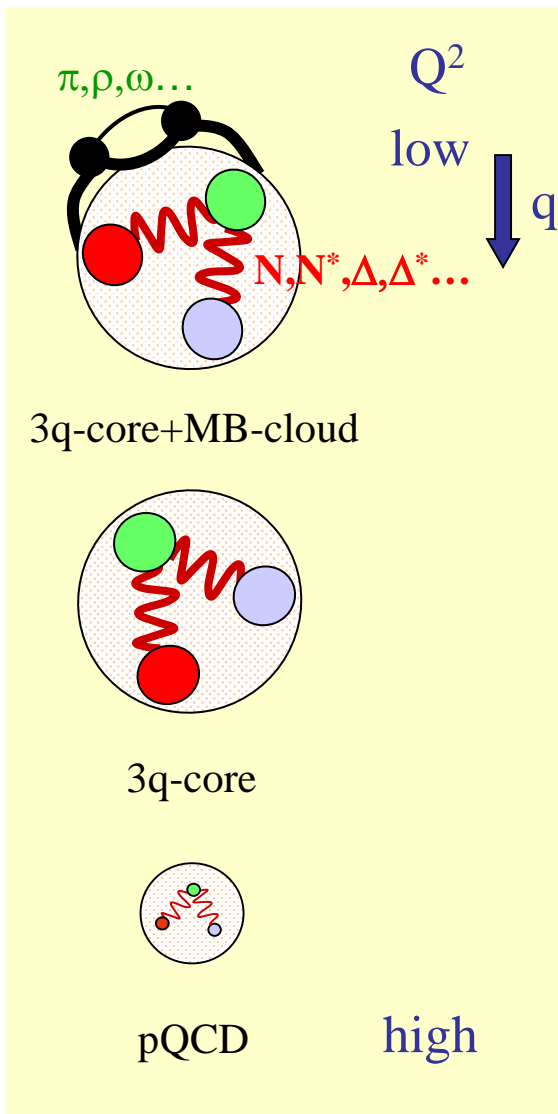
# Emergence of Hadron Mass Traced by Electromagnetic Probes



➤ Study the structure of the nucleon spectrum in the domain where dressed quarks are the major active degree of freedom.

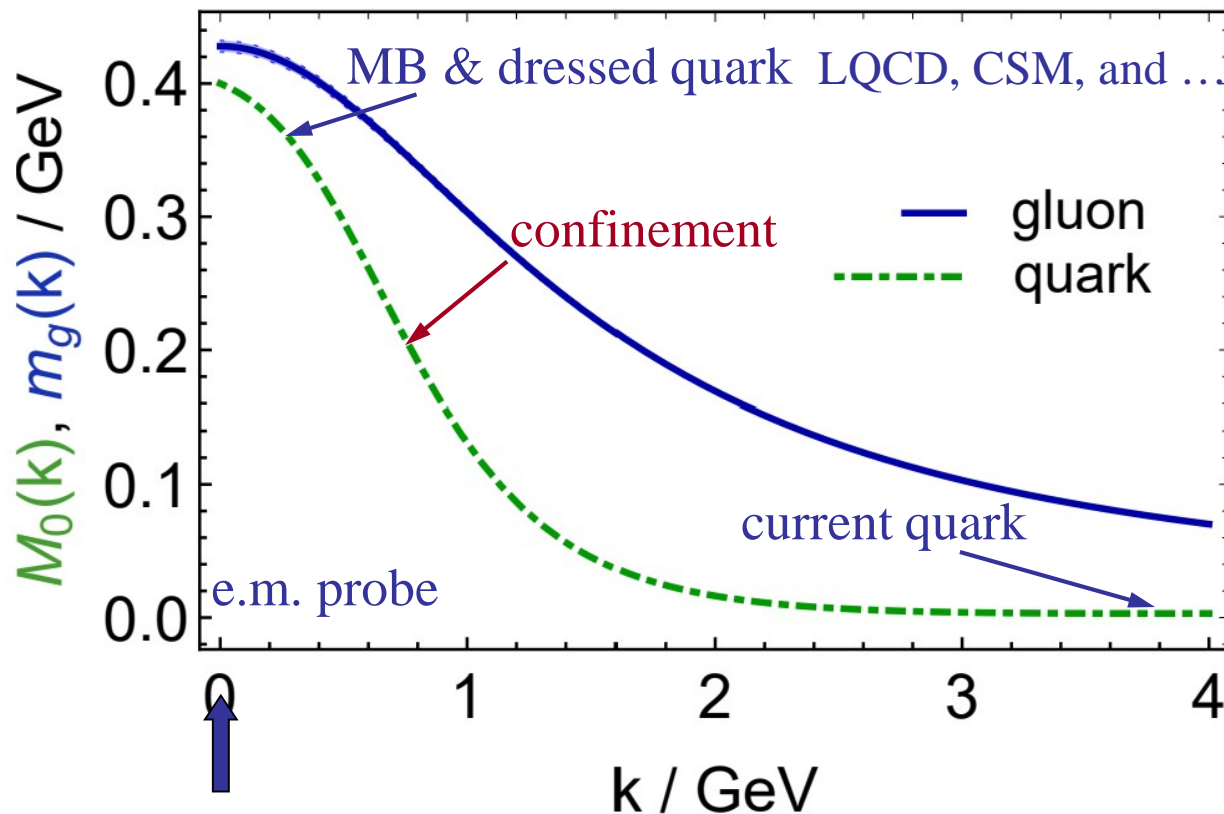


# Emergence of Hadron Mass Traced by Electromagnetic Probes



➤ Study the structure of the nucleon spectrum in the domain where most of the mass is generated by the strong field and dressed quarks are the major active degree of freedom.

Zhu-Fang Cui et al., Chin. Phys. C **44** (2020) 083102/1-10

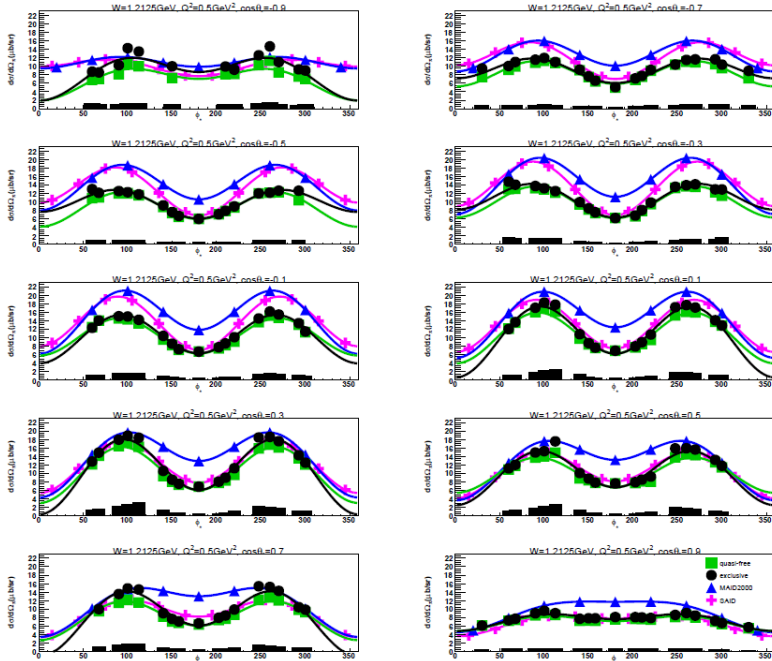


# CLAS

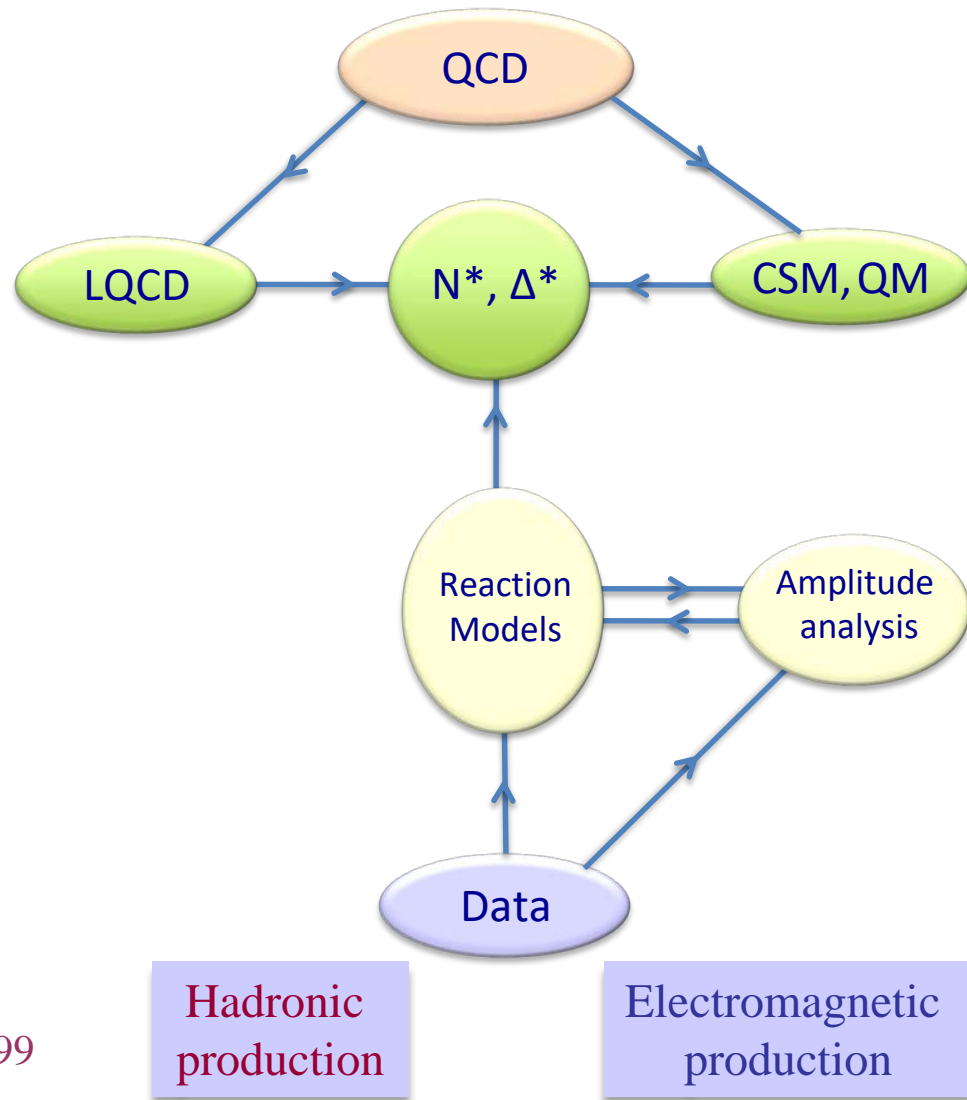
# Data-Driven Data Analyses

## Consistent Results

Single Pion



Int. J. Mod. Phys. E, Vol. 22, 1330015 (2013) 1-99



Hadronic production

Electromagnetic production

# Exclusive Single $\pi^-$ Electroproduction off the Deuteron

Y. Tian *et al.*, Phys. Rev. C **107**, 015201 (2023) 26

$W = 1.2125$  GeV

$\Delta W = 25$  MeV

$Q^2 = 0.5$  GeV<sup>2</sup>

$\Delta Q^2 = 0.2$  GeV<sup>2</sup>

$\cos(\theta) = -0.7$

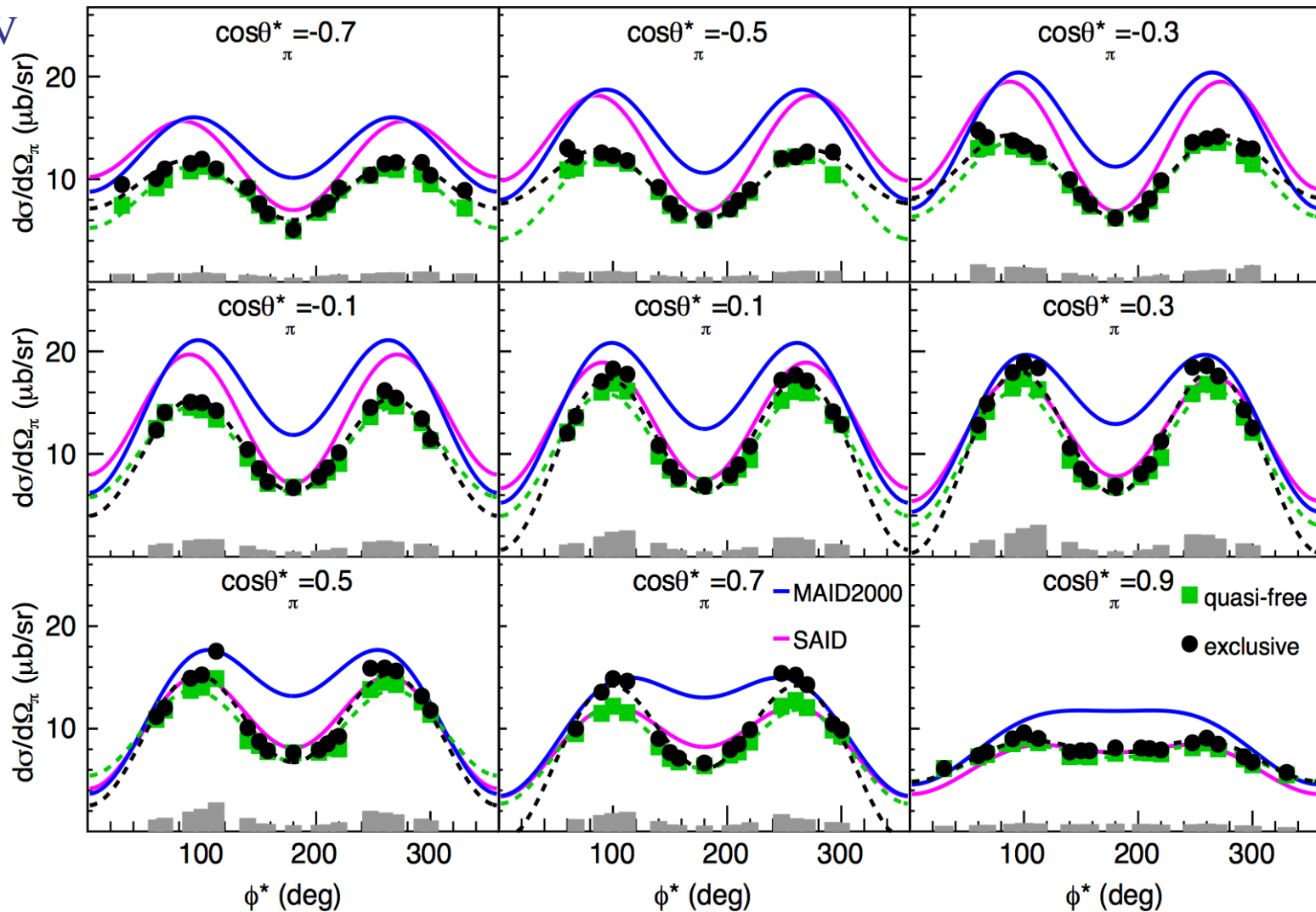
$\Delta\cos(\theta) = 0.2$

$\cos(\theta) = 0.9$

$\phi = 20^\circ$

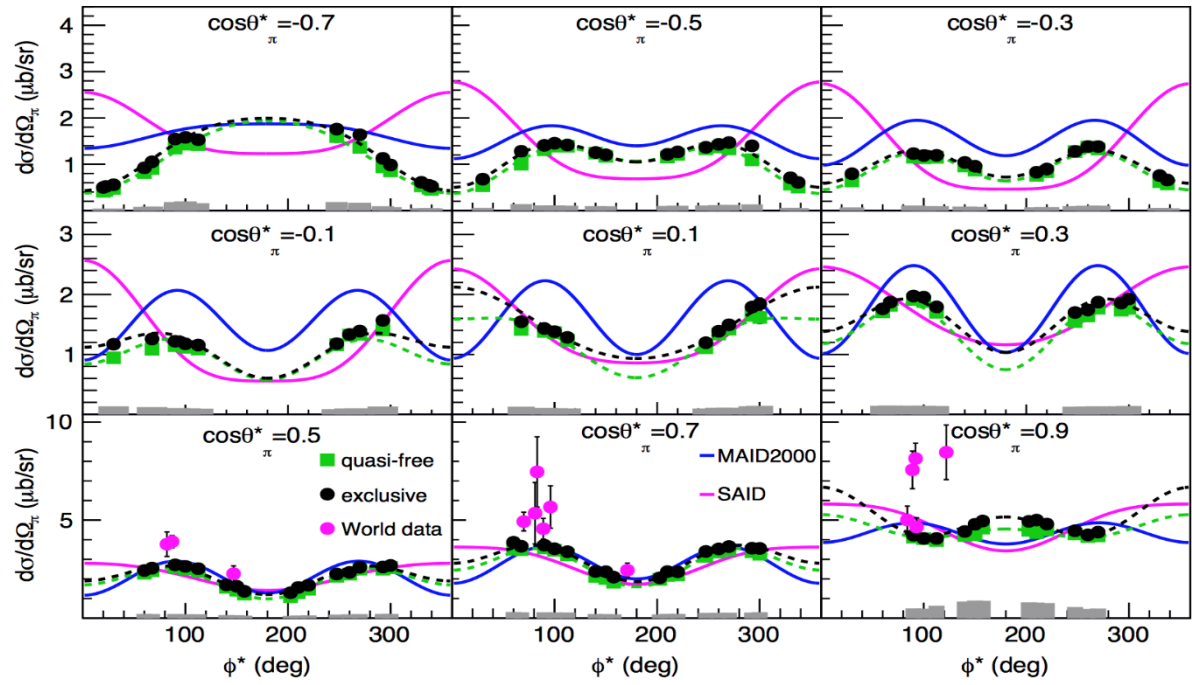
$\Delta\phi = 40^\circ$

$\phi = 340^\circ$



# Exclusive Single $\pi^-$ Electroproduction off the Deuteron

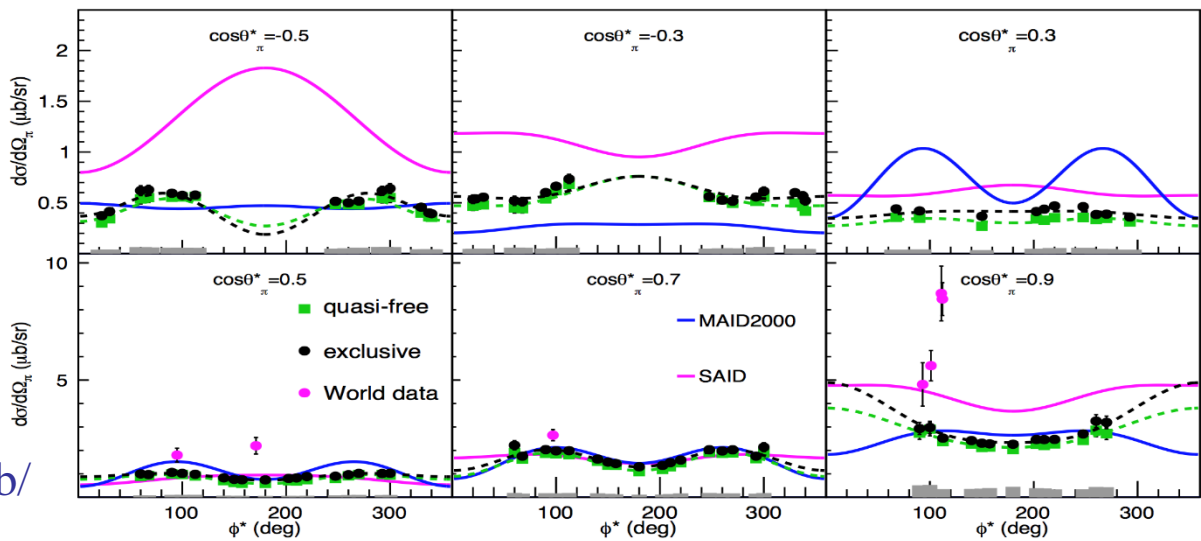
Ye Tian



W = 1.5125 GeV

$Q^2 = 0.5 \text{ GeV}^2$   
 $\Delta Q^2 = 0.2 \text{ GeV}^2$

W = 1.6625 GeV



CLAS Database:

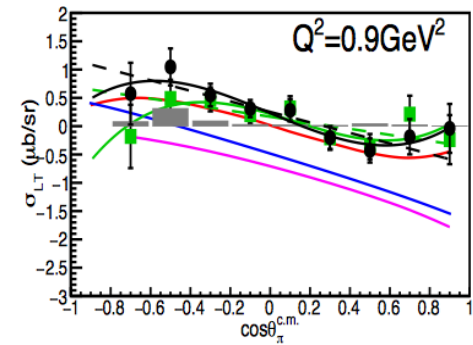
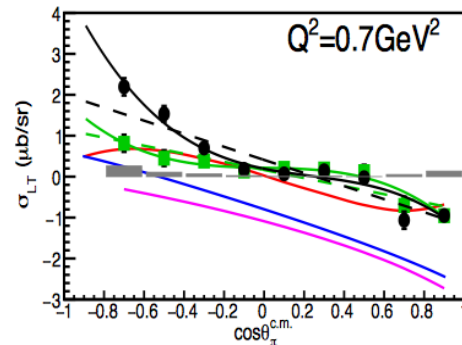
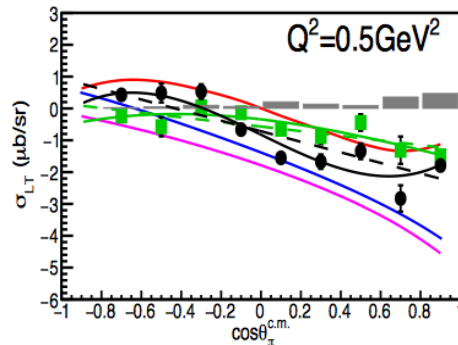
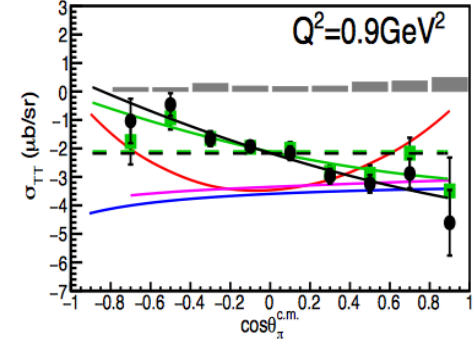
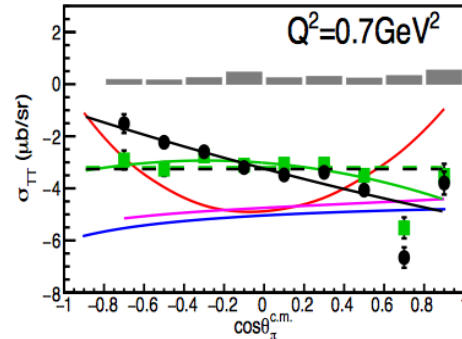
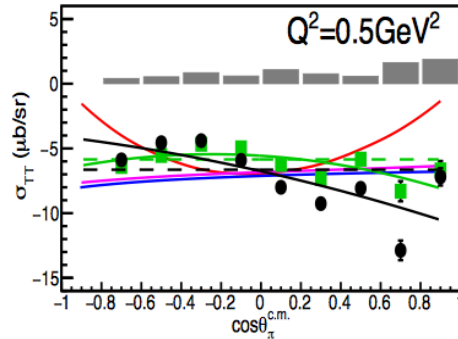
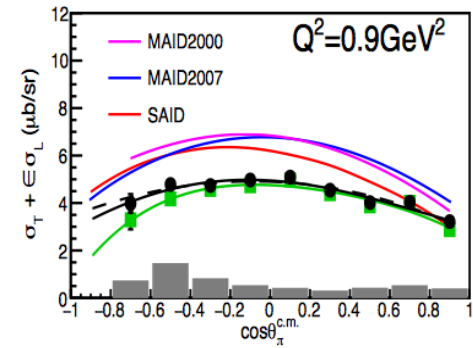
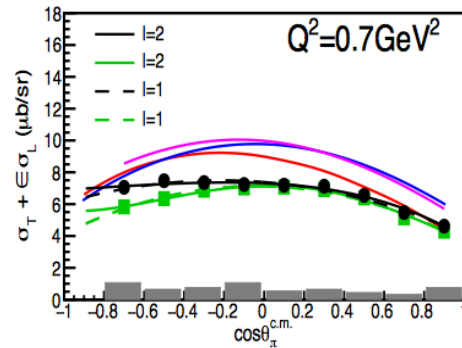
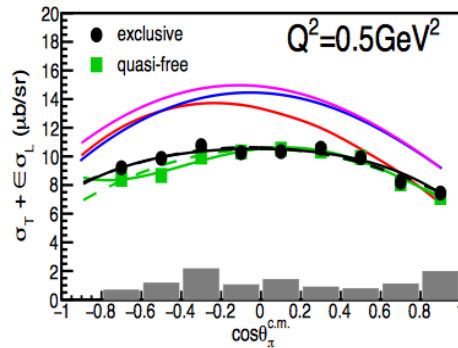
<https://clasweb.jlab.org/physicsdb/>



# $\cos \theta_\pi$ -Dependent Structure Functions @ $W=1.2125$ GeV

$W = 1.2125$  GeV     $\Delta W = 25$  MeV

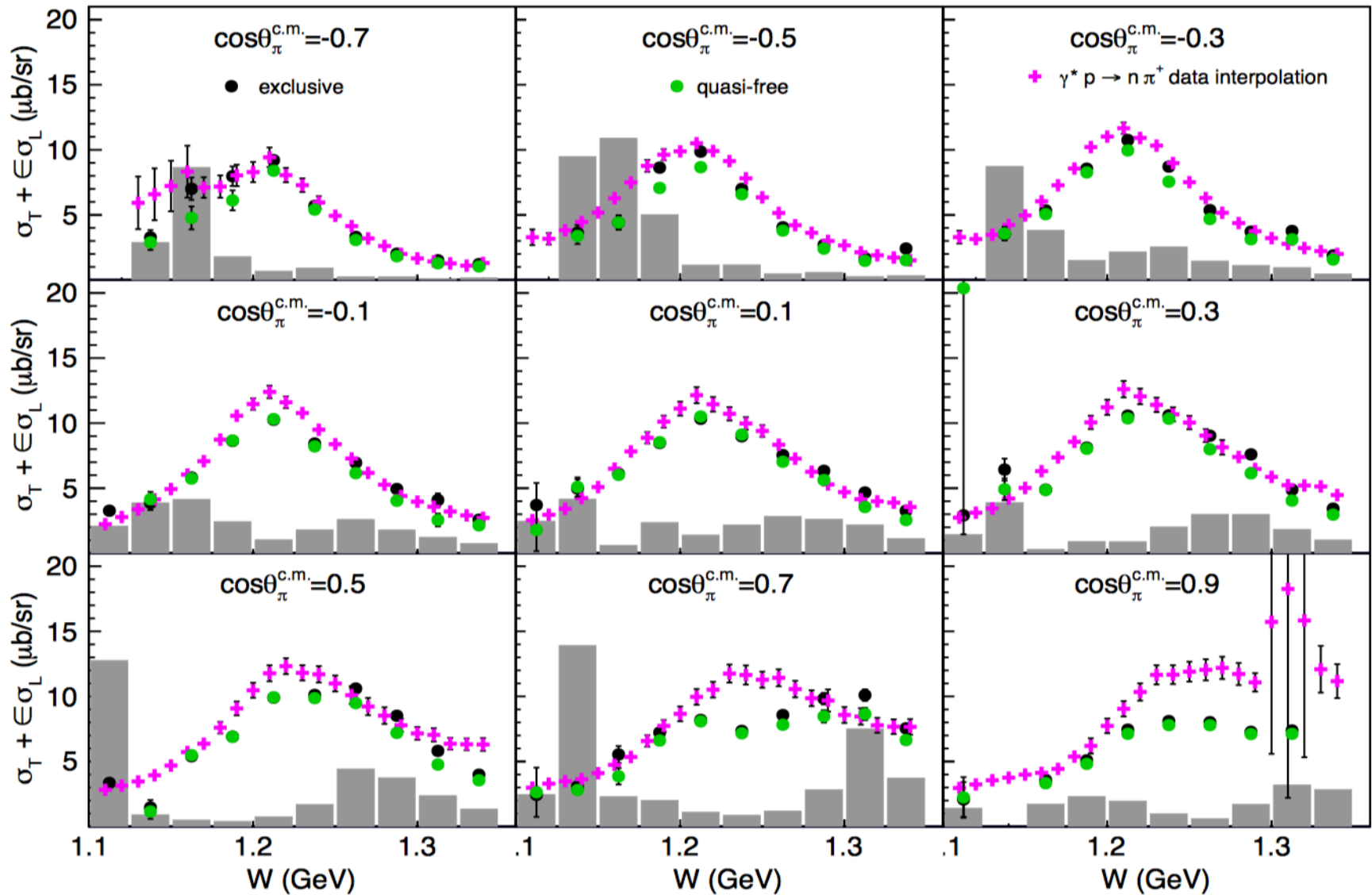
Ye Tian



# W-Dependent of the Structure Function $\sigma_T + \epsilon\sigma_L$

$Q^2 = 0.5 \text{ GeV}^2$      $\Delta Q^2 = 0.2 \text{ GeV}^2$

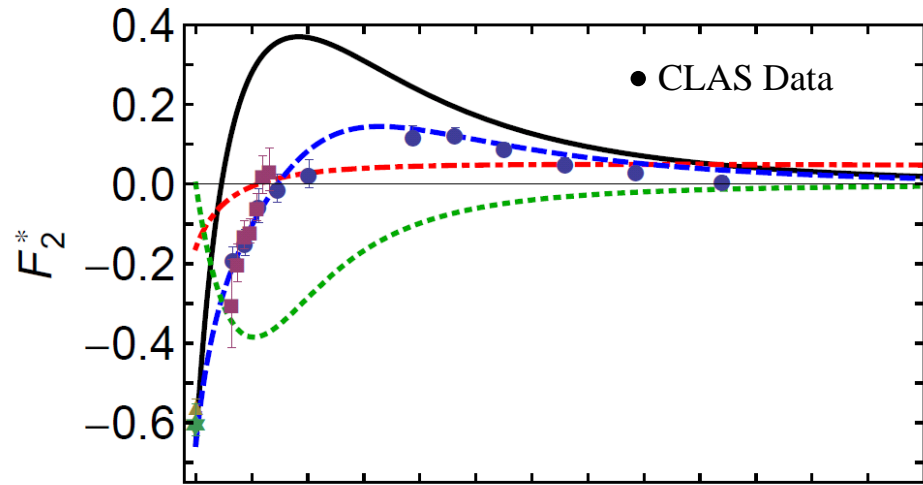
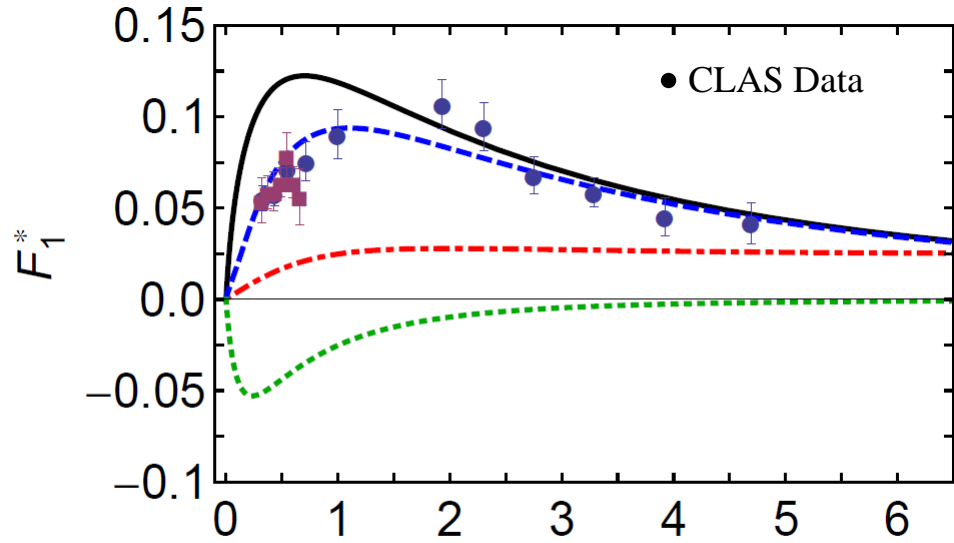
Ye Tian



# Roper Transition Form Factors in CSM Approach

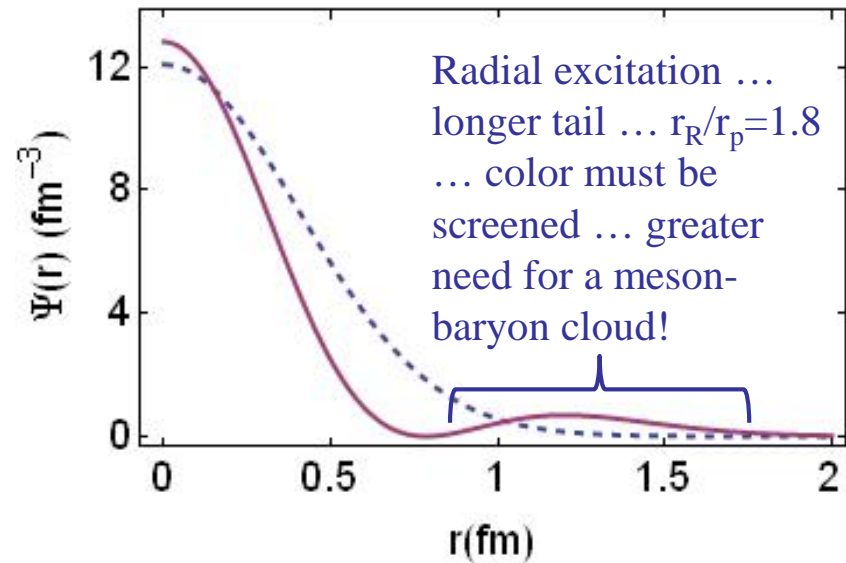
$N(1440)P_{11}$

J. Segovia *et al.*, Phys. Rev. Lett. 115, 171801 (2015)



- DSE Contact  $x=Q^2/m_N^2$
- DSE Realistic
- Inferred meson-cloud contribution
- Anticipated complete result

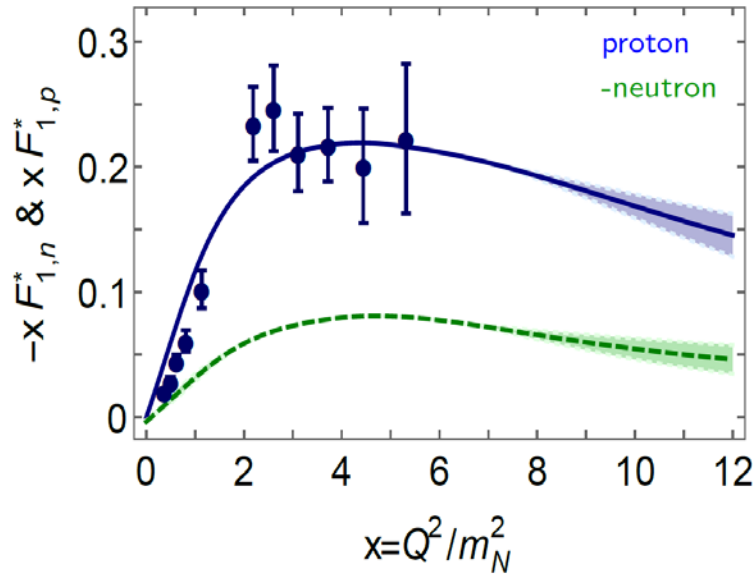
Importantly, the existence of a zero in  $F_2$  is not influenced by meson-cloud effects, although its precise location is.



# Roper Transition Form Factors in CSM Approach

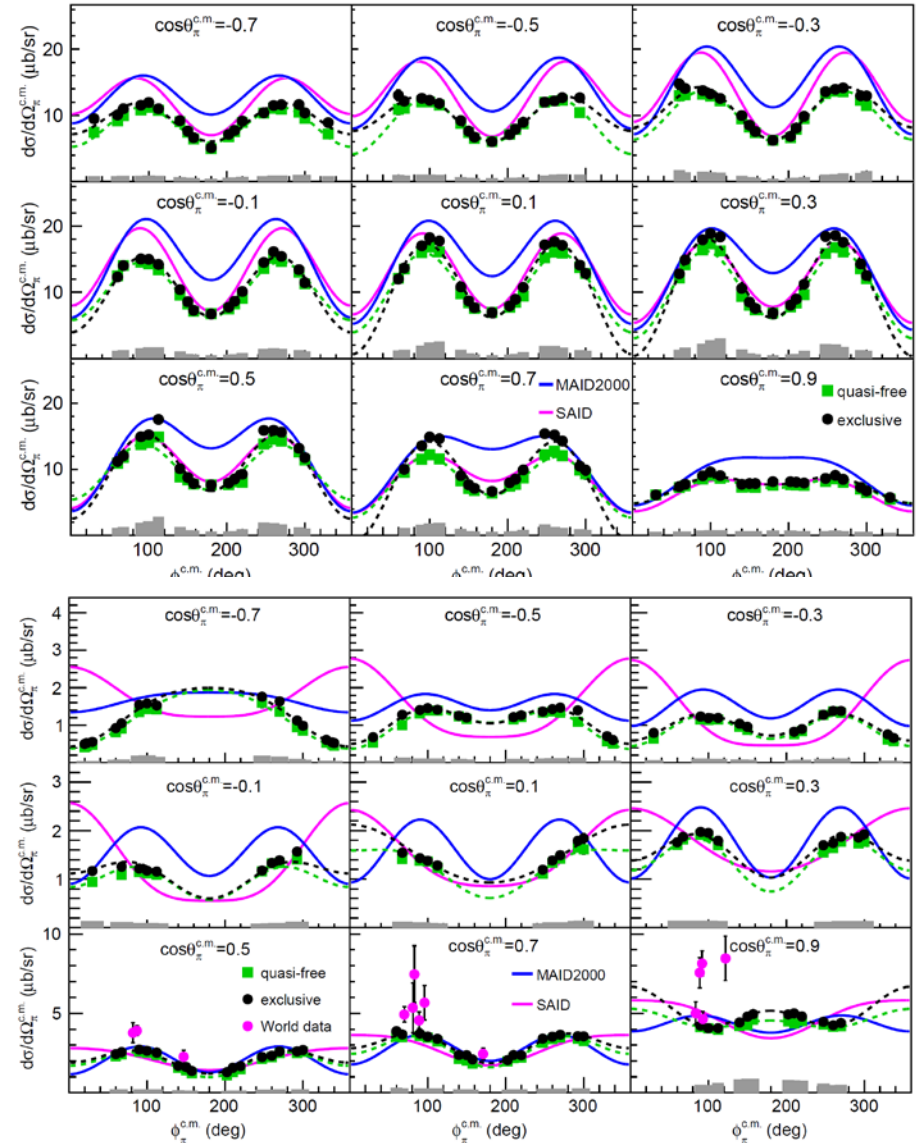
$N(1440)P_{11}$

Y. Tian *et al.*, Phys. Rev. C **107**, 015201 (2023) 26



$W = 1.2125 \text{ GeV}$

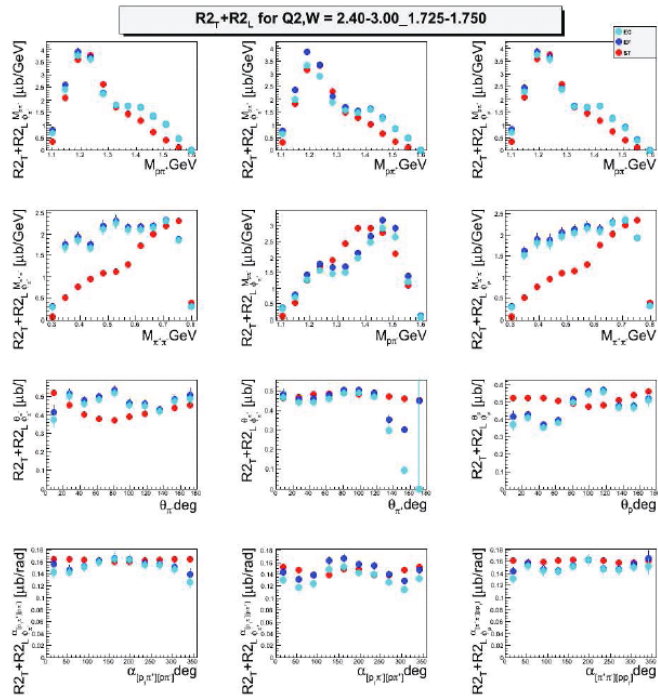
$W = 1.5125 \text{ GeV}$



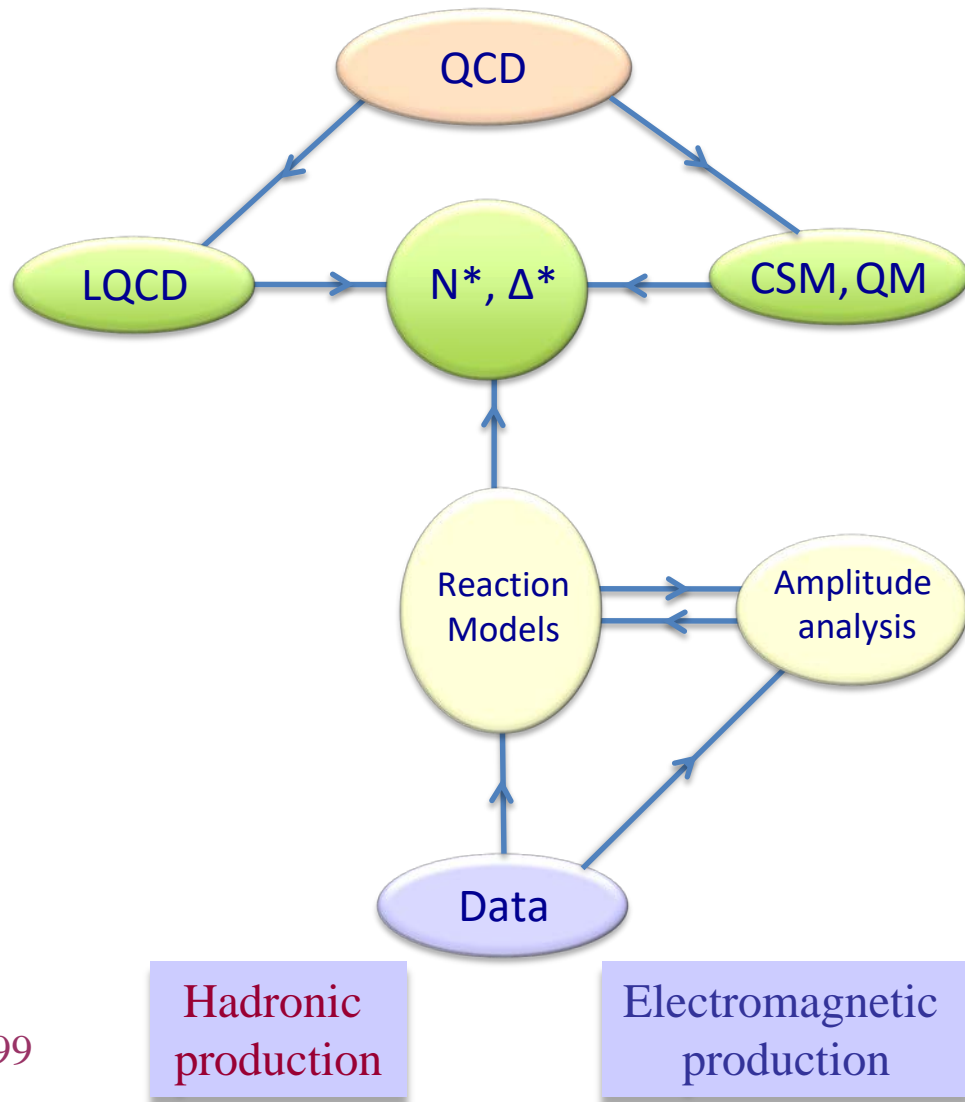
# Data-Driven Data Analyses

## Consistent Results

Double Pion



Int. J. Mod. Phys. E, Vol. 22, 1330015 (2013) 1-99



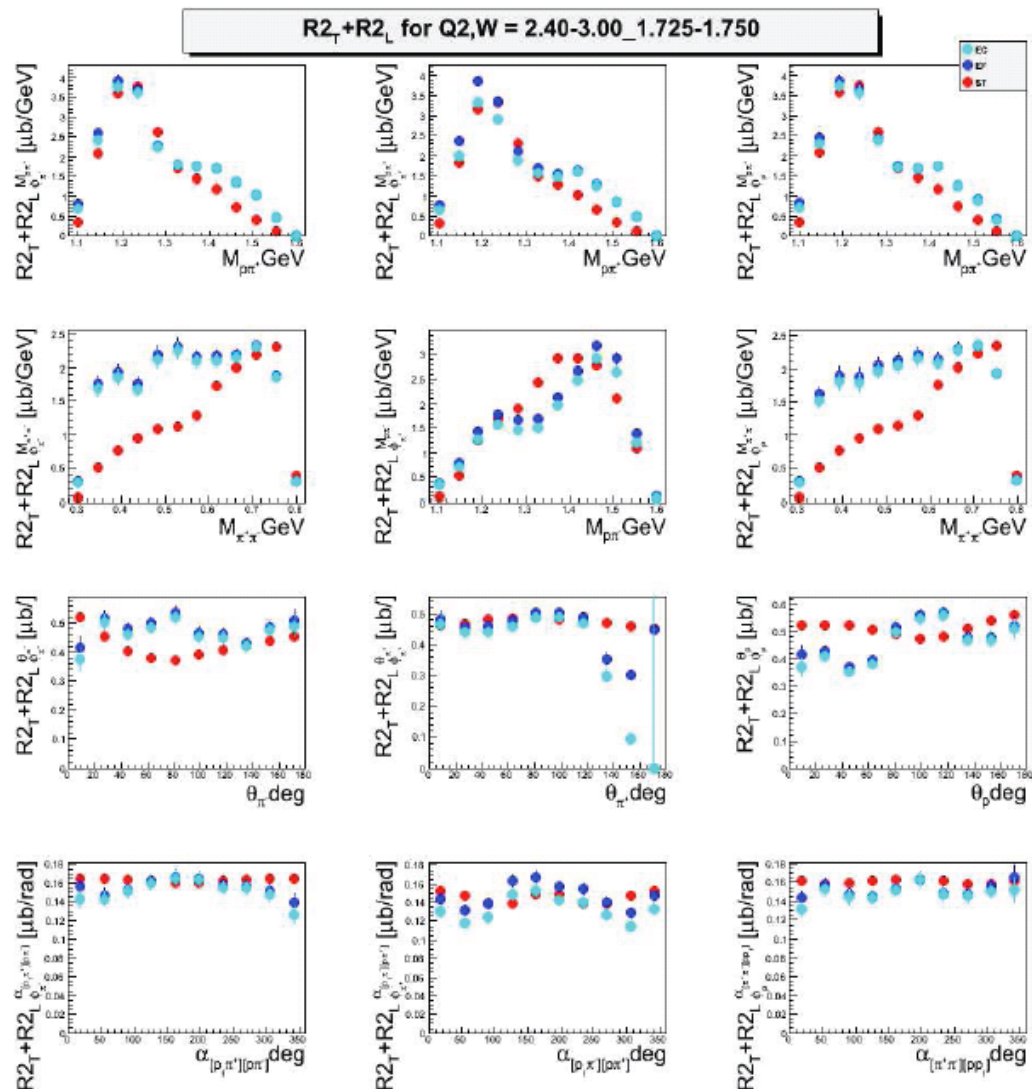
Hadronic production

Electromagnetic production

# $\phi$ -independent $N\pi\pi$ Single-Differential Cross Sections

$Q^2, W$  bin =  $[2.4, 3.0) \text{ GeV}^2, [1.725, 1.750) \text{ GeV}$

Arjun Trivedi  
Evgeny Isupov



● normalized

● hole filled

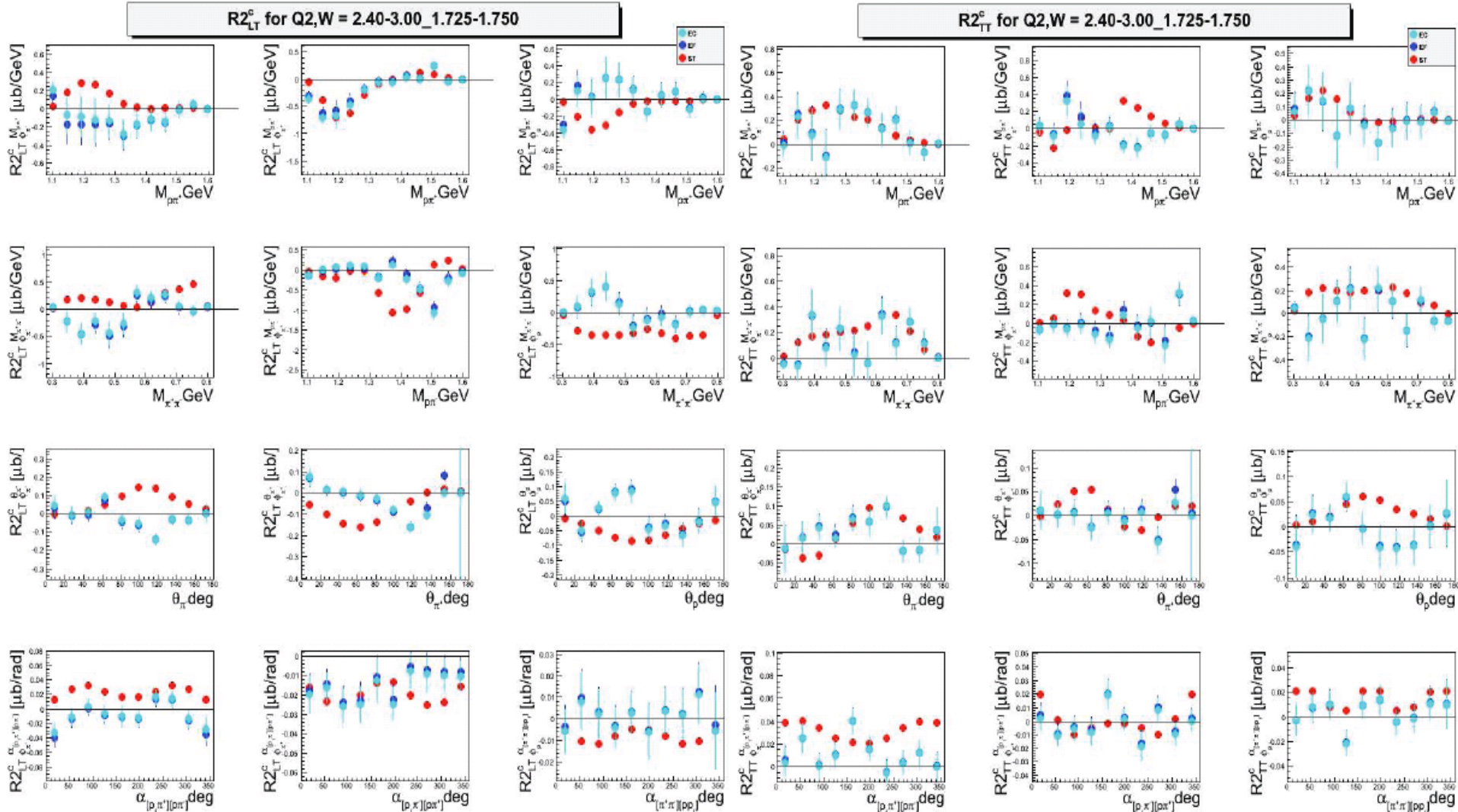
● TWOPEG

$$\left( \frac{d^2\sigma}{dX_{ij}d\phi_i} \right) = \underline{R2_T} X_{ij} + \underline{R2_L} X_{ij} + R2_{LT}^{c, X_{ij}} \cos \phi_i + R2_{TT}^{c, X_{ij}} \cos 2\phi_i + \delta_{X_{ij}\alpha_i} (R2_{LT}^{s, \alpha_i} \sin \phi_i + R2_{TT}^{s, \alpha_i} \sin 2\phi_i)$$

# $\phi$ -dependent $N\pi\pi$ Single-Differential Cross Sections

$Q^2, W$  bin =  $[2.4, 3.0)\text{GeV}^2, [1.725, 1.750)\text{GeV}$

Arjun Trivedi



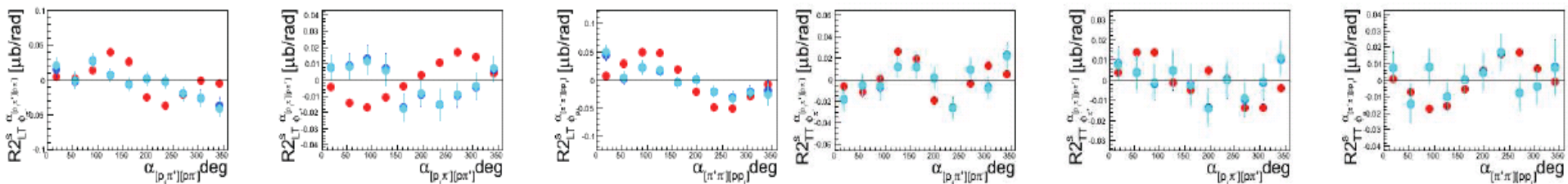
$$\left( \frac{d^2\sigma}{dX_{ij}d\phi_i} \right) = R2_T^{X_{ij}} + R2_L^{X_{ij}} + \underline{R2_{LT}^{c, X_{ij}} \cos \phi_i} + \underline{R2_{TT}^{c, X_{ij}} \cos 2\phi_i} + \delta_{X_{ij}\alpha_i} (R2_{LT}^{s, \alpha_i} \sin \phi_i + R2_{TT}^{s, \alpha_i} \sin 2\phi_i)$$

# $\phi$ -dependent $N\pi\pi$ Single-Differential Cross Sections

$Q^2, W$  bin =  $[2.4, 3.0) \text{ GeV}^2, [1.725, 1.750) \text{ GeV}$

Arjun Trivedi

Chris McLauchlin extracts the **beam helicity dependent** differential cross sections.



$$\left( \frac{d^2\sigma}{dX_{ij}d\phi_i} \right) = R2_T^{X_{ij}} + R2_L^{X_{ij}} + R2_{LT}^{c, X_{ij}} \cos \phi_i + R2_{TT}^{c, X_{ij}} \cos 2\phi_i + \delta_{X_{ij}\alpha_i} \left( \underline{R2_{LT}^{s, \alpha_i} \sin \phi_i} + \underline{R2_{TT}^{s, \alpha_i} \sin 2\phi_i} \right)$$



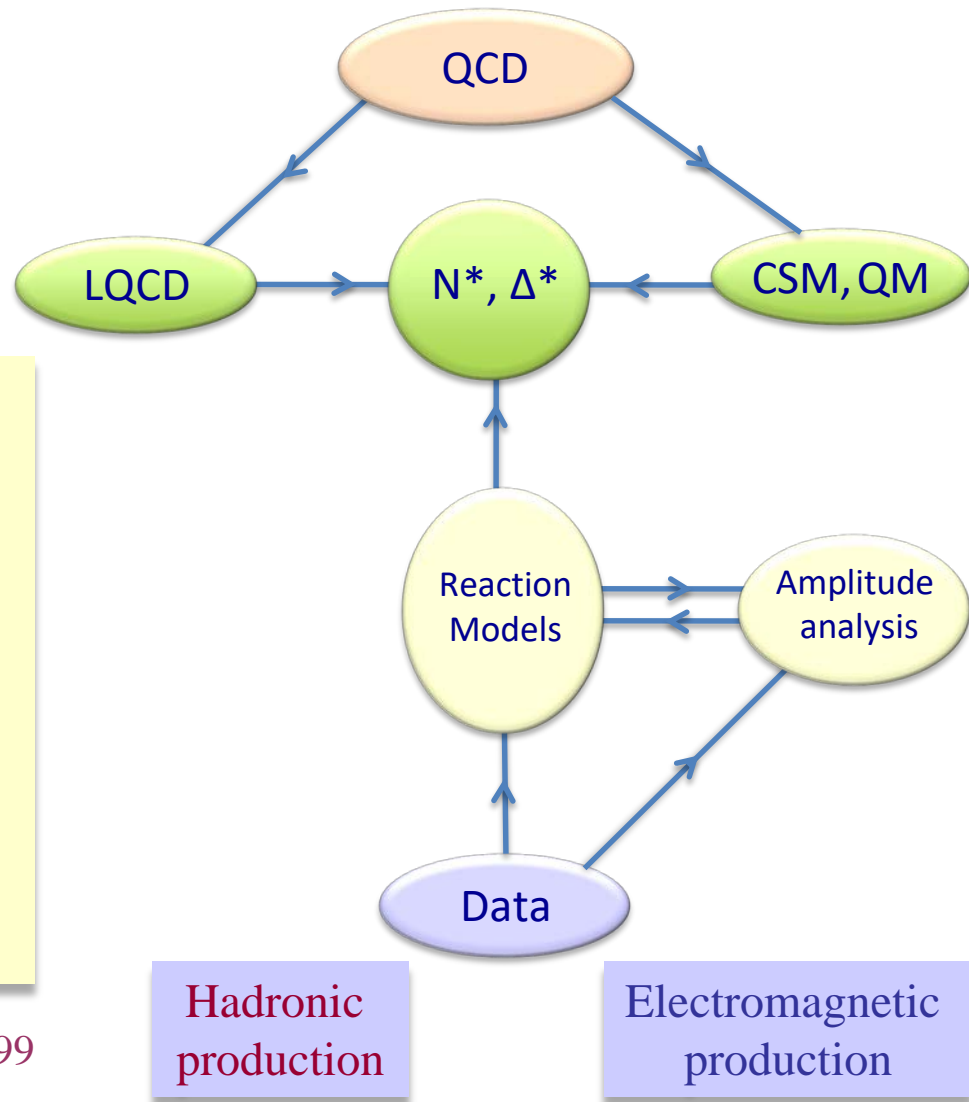
# Data-Driven Data Analyses

## Consistent Results



- Single meson production:  
Unitary Isobar Model (UIM)  
Fixed- $t$  Dispersion Relations (DR)
- Double pion production:  
Unitarized Isobar Model (JM)
- Coupled-Channel Approaches:  
EBAC  $\Rightarrow$  Argonne-Osaka  
JAW  $\Rightarrow$  Jülich-Athens-Washington  $\Rightarrow$  JüBo  
BoGa  $\Rightarrow$  Bonn-Gatchina

Int. J. Mod. Phys. E, Vol. 22, 1330015 (2013) 1-99

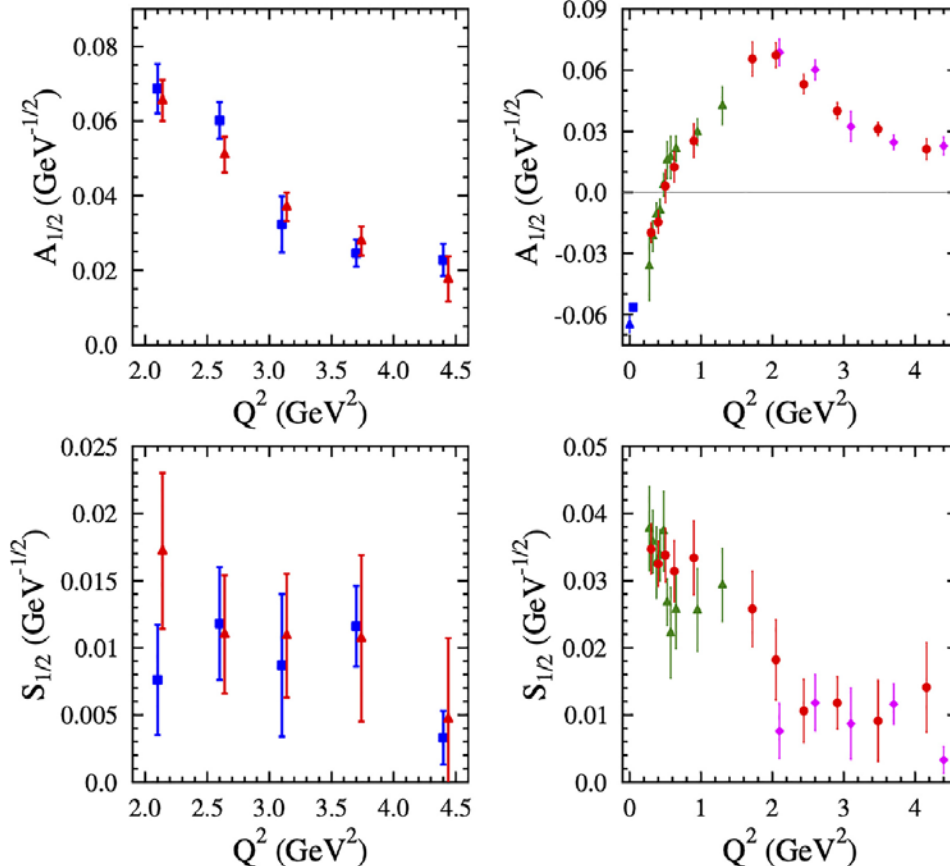


Hadronic  
production

Electromagnetic  
production

# N(1440)1/2<sup>+</sup> Couplings from CLAS

Viktor Mokeev



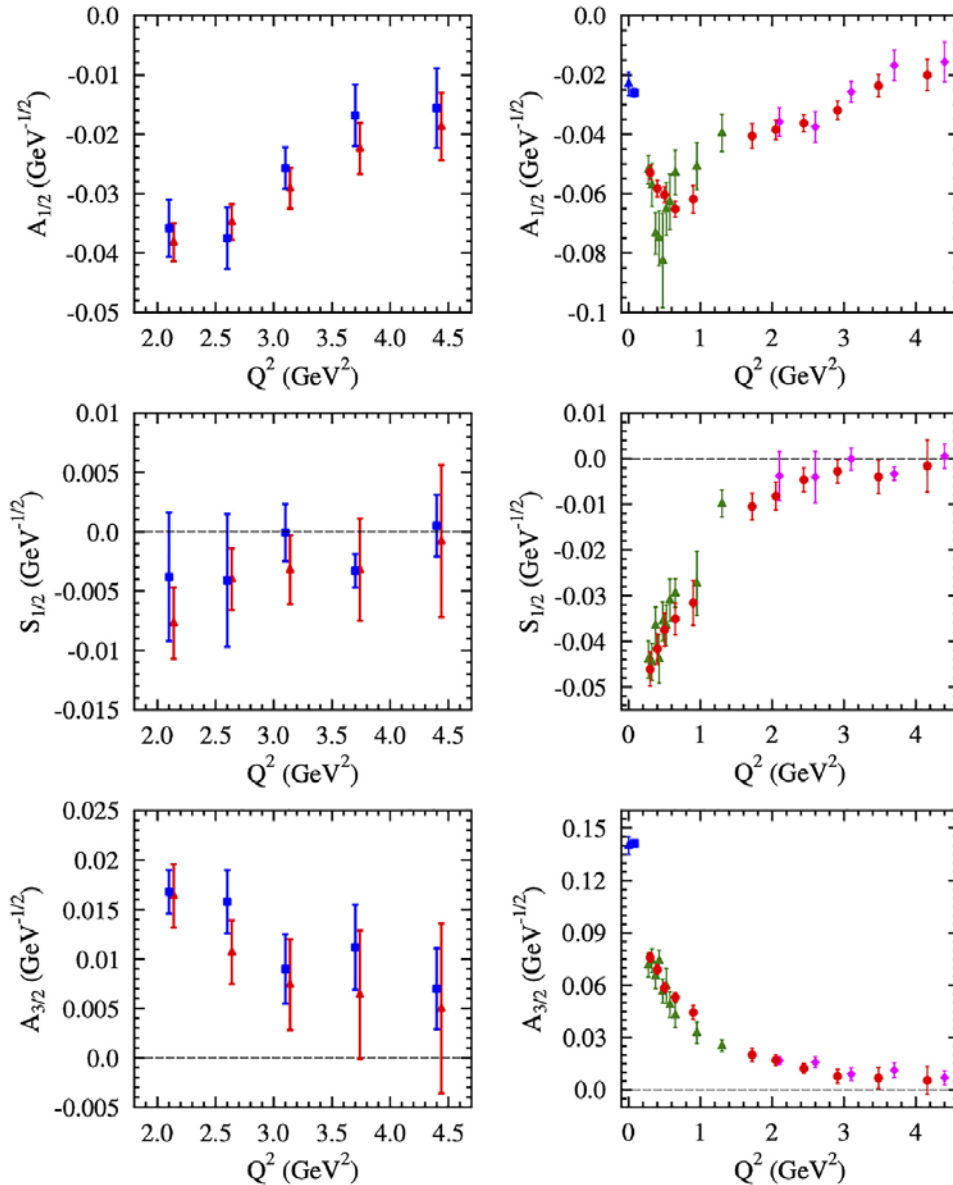
Consistent results are now obtained in the low-lying resonance region up to a  $Q^2$  of 5 GeV<sup>2</sup> by independent analyses from the  $N\pi$  differential cross sections, beam, target, and beam-target asymmetries (red triangles) and  $p\pi^+\pi^-$  differential cross sections (blue squares).

All observables have fundamentally different mechanisms for the nonresonant background and underscore the capability of the reaction models to extract reliable resonance electrocouplings.

Phys. Rev. C 108, 025204 (2023) 1-26

# N(1520) 3/2<sup>-</sup> Couplings from CLAS

Viktor Mokeev



Consistent results are now obtained in the low-lying resonance region up to a  $Q^2$  of 5 GeV<sup>2</sup> by **independent analyses** from the  $N\pi$  differential cross sections, beam, target, and beam-target asymmetries (**red triangles**) and  $p\pi^+\pi^-$  differential cross sections (**blue squares**).

All observables have **fundamentally different mechanisms** for the **nonresonant background** and underscore the capability of the reaction models to extract reliable resonance electrocouplings.

Phys. Rev. C 108, 025204 (2023) 1-26

# New $N'(1720)3/2^+$ State and its Properties


$N^*$  hadronic decays from JM15 that incorporates  $N'(1720)3/2^+$

| Resonance                                                   | BF( $\pi\Delta$ ), % | BF( $\rho p$ ), % |
|-------------------------------------------------------------|----------------------|-------------------|
| $N'(1720)3/2^+$<br>electroproduction<br>photoproduction     | 47-64<br>46-62       | 3-10<br>4-13      |
| $N(1720)3/2^+$<br>electroproduction<br>photoproduction      | 39-55<br>38-53       | 23-49<br>31-46    |
| $\Delta(1700)3/2^-$<br>electroproduction<br>photoproduction | 77-95<br>78-93       | 3-5<br>3-6        |

A successful description of  $\pi^+\pi^-p$  photo- and electro-production cross sections at  $Q^2=0, 0.65, 0.95,$  and  $1.30 \text{ GeV}^2$  has been achieved by implementing a new  $N'(1720)3/2^+$  state with  $Q^2$ -independent hadronic decay widths of all resonances that contribute at  $W \sim 1.7 \text{ GeV}$ , that allows us to claim the existence of a new  $N'(1720)3/2^+$  state.


Mass: 1.715-1.735 GeV

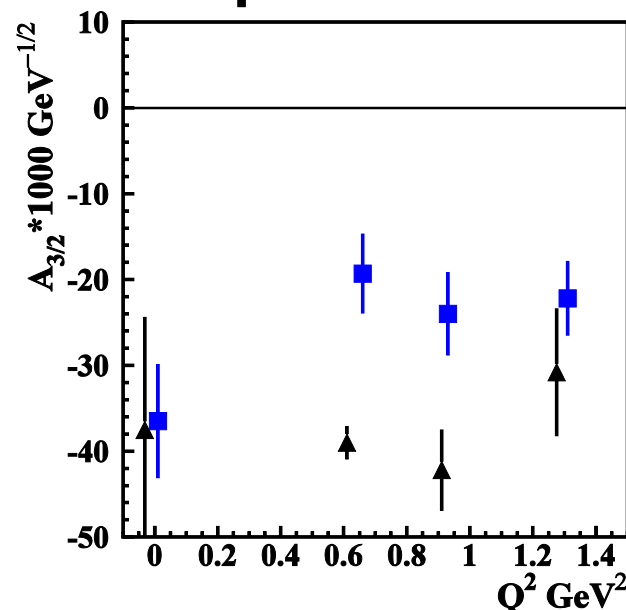
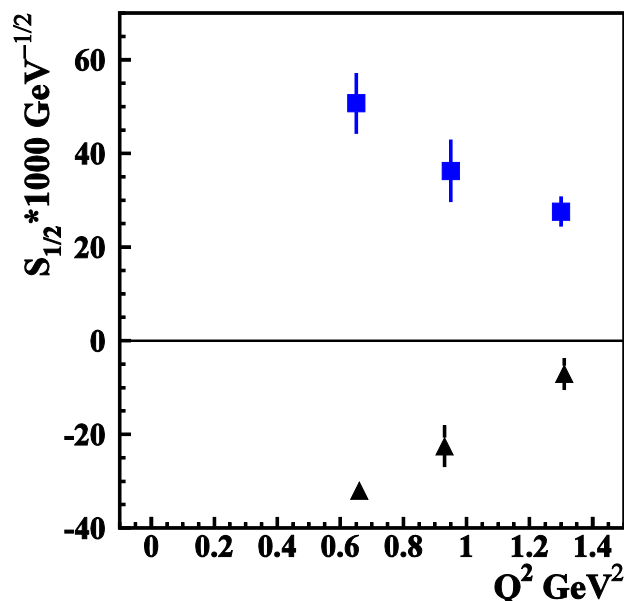
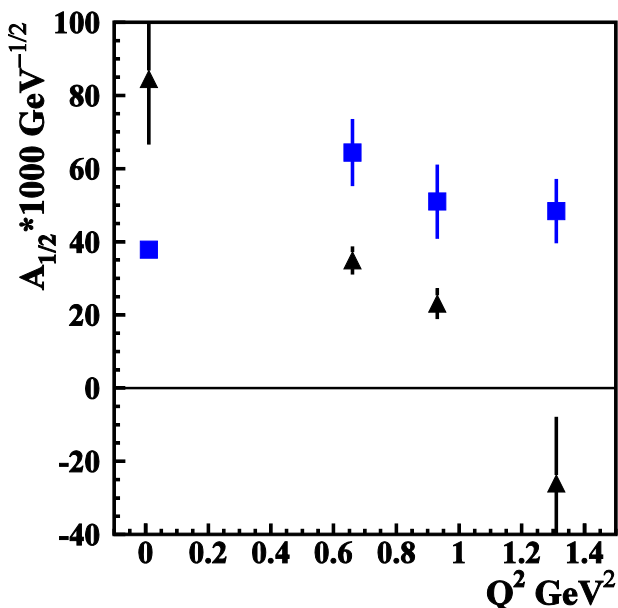
Width:  $120 \pm 6 \text{ MeV}$

  $N'(1720)3/2^+$

Mass: 1.743-1.753 GeV

Width:  $112 \pm 8 \text{ MeV}$

  $N(1720)3/2^+$



# New $N'(1720)3/2^+$ State and its Properties

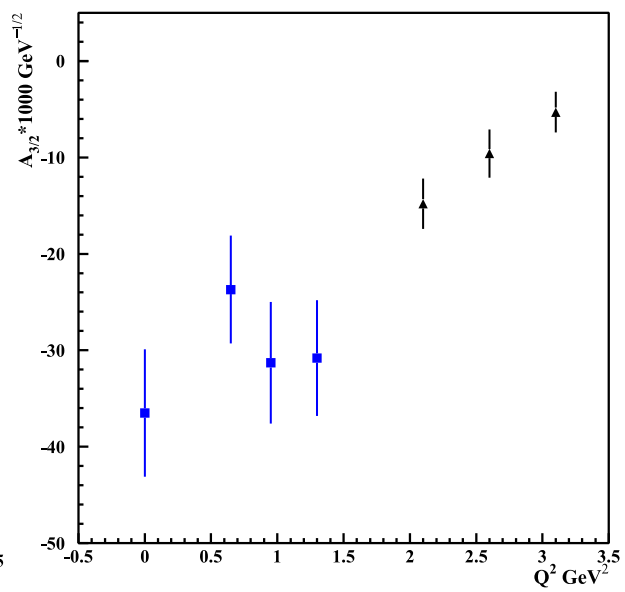
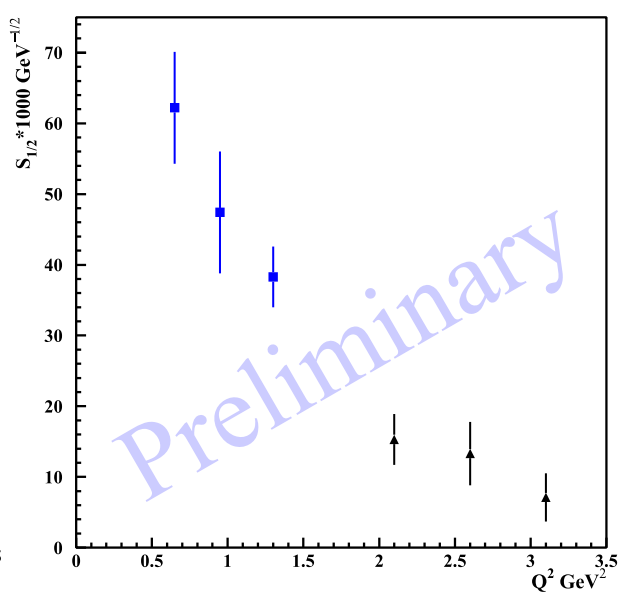
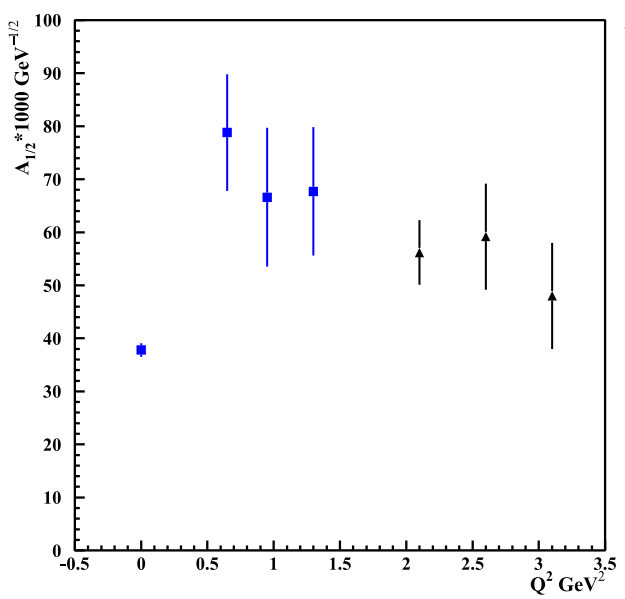
$N^*$  hadronic decays from JM15 that incorporates  $N'(1720)3/2^+$

| Resonance                                                   | BF( $\pi\Delta$ ), % | BF( $\rho p$ ), % |
|-------------------------------------------------------------|----------------------|-------------------|
| $N'(1720)3/2^+$<br>electroproduction<br>photoproduction     | 47-64<br>46-62       | 3-10<br>4-13      |
| $N(1720)3/2^+$<br>electroproduction<br>photoproduction      | 39-55<br>38-53       | 23-49<br>31-46    |
| $\Delta(1700)3/2^-$<br>electroproduction<br>photoproduction | 77-95<br>78-93       | 3-5<br>3-6        |

A successful description of  $\pi^+\pi^-p$  photo- and electro-production cross sections at  $Q^2=0, 0.65, 0.95,$  and  $1.30 \text{ GeV}^2$  has been achieved by implementing a new  $N'(1720)3/2^+$  state with  $Q^2$ -independent hadronic decay widths of all resonances that contribute at  $W \sim 1.7 \text{ GeV}$ , that allows us to claim the existence of a new  $N'(1720)3/2^+$  state.

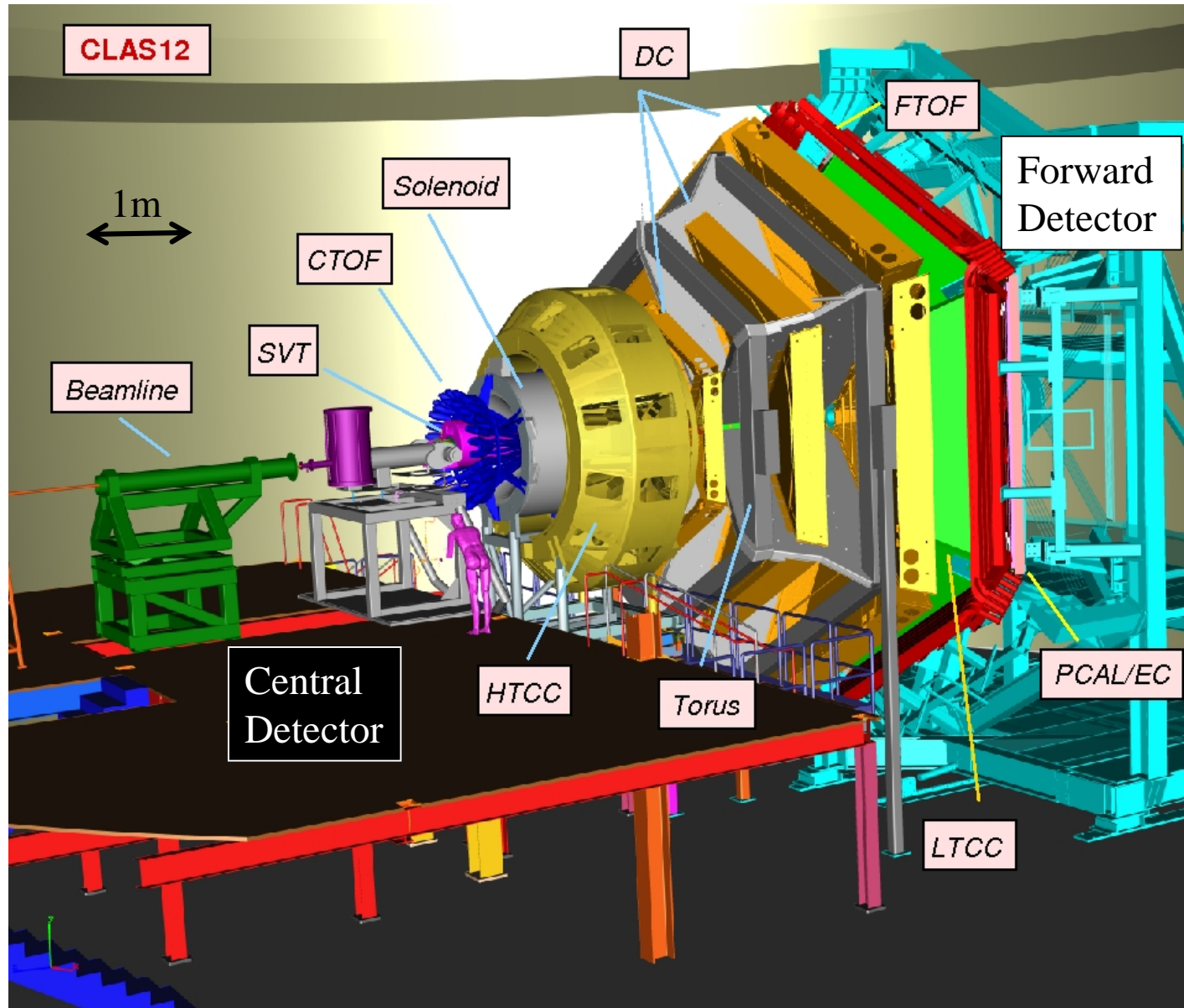
Mass: 1.715-1.735 GeV  
Width:  $120 \pm 6 \text{ MeV}$   
 $N'(1720)3/2^+$

May 2024  
update



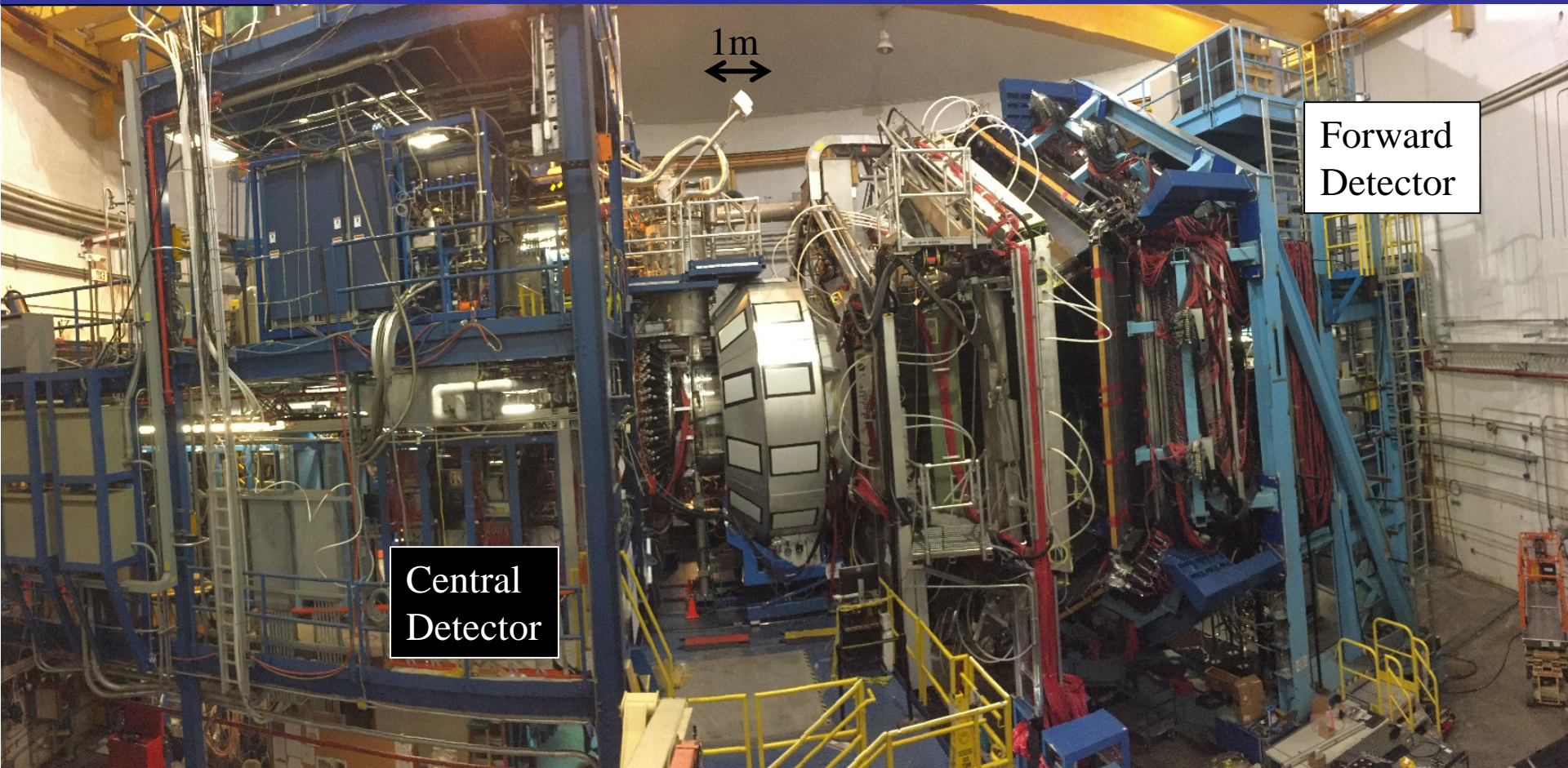
# CLAS12

# CLAS12



- Luminosity  $> 10^{35} \text{ cm}^{-2} \text{ s}^{-1}$
- Hermeticity
- Polarization
  
- Baryon Spectroscopy
- Elastic Form Factors
- $N \rightarrow N^*$  Form Factors
- GPDs and TMDs
- DIS and SIDIS
- Nucleon Spin Structure
- Color Transparency
- ...

# CLAS12



- Luminosity  $>10^{35} \text{ cm}^{-2}\text{s}^{-1}$
- Hermeticity
- Polarization

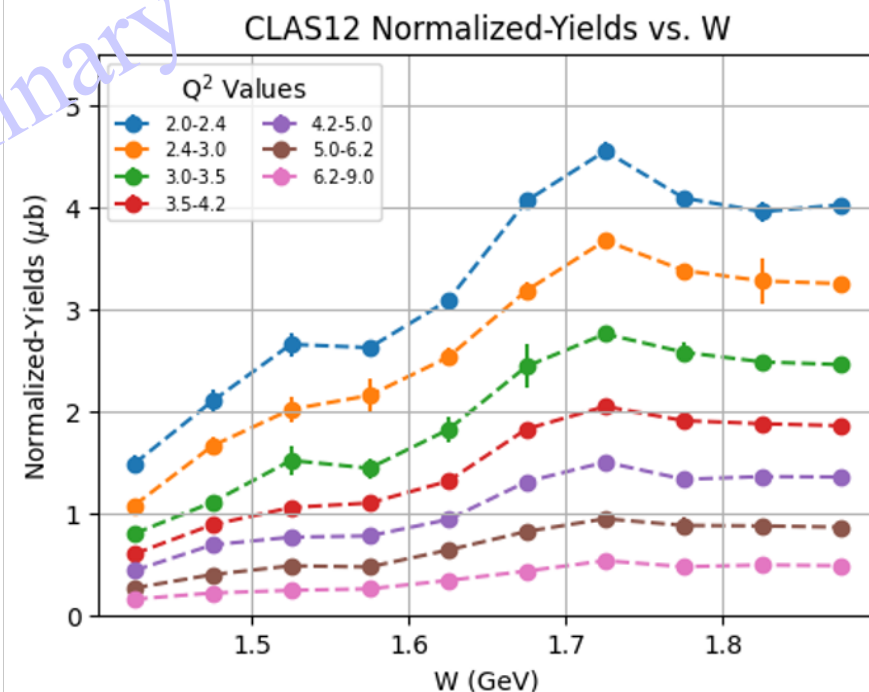
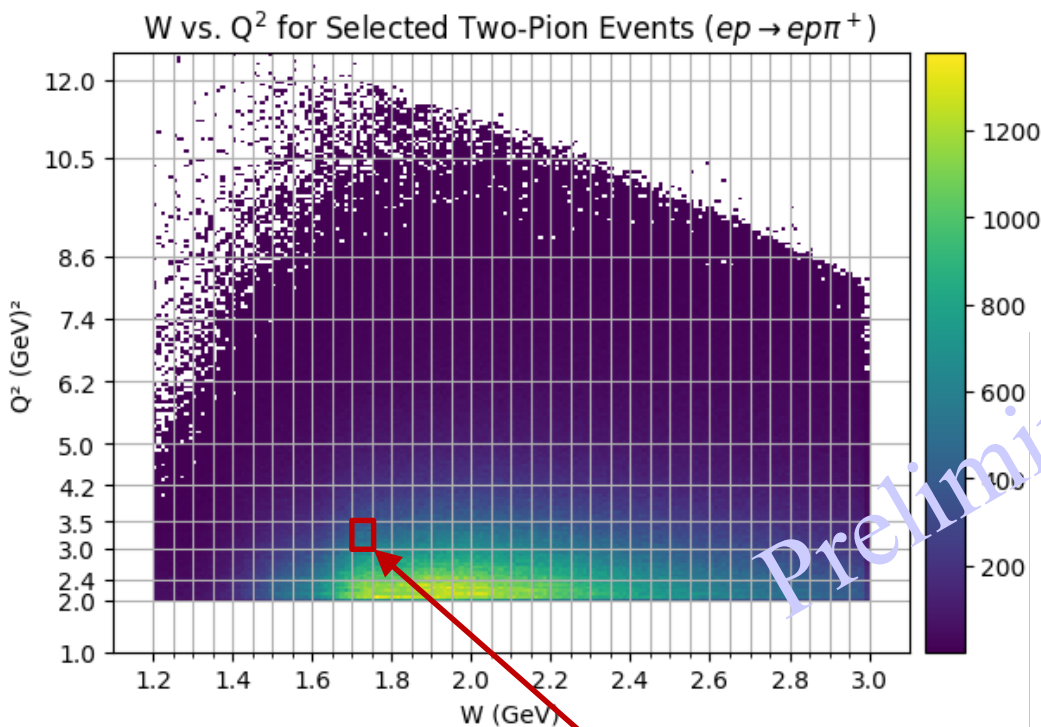
- Baryon Spectroscopy
- Elastic Form Factors
- $N \rightarrow N^*$  Form Factors

- GPDs and TMDs
- DIS and SIDIS
- Nucleon Spin Structure
- Color Transparency
- ...



# Preliminary RGA CLAS12 Data Analysis: $p\pi^+\pi^-$

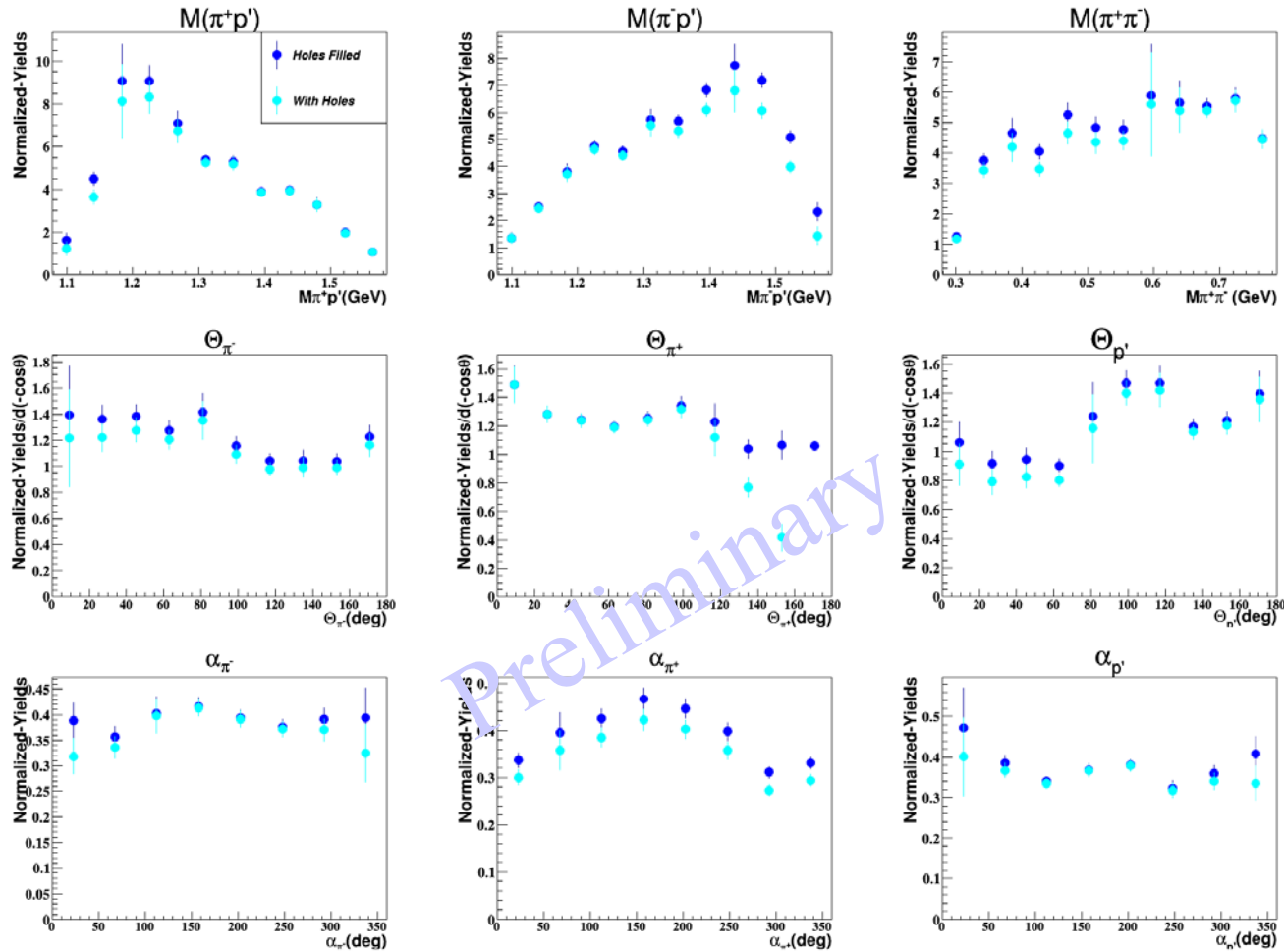
Krishna Neupane  
CLAS12



$1.725 \text{ GeV} < W < 1.75 \text{ GeV}$  and  $3 \text{ GeV}^2 < Q^2 < 3.5 \text{ GeV}^2$

# Preliminary RGA CLAS12 Data Analysis: $p\pi^+\pi^-$

Krishna Neupane  
CLAS12

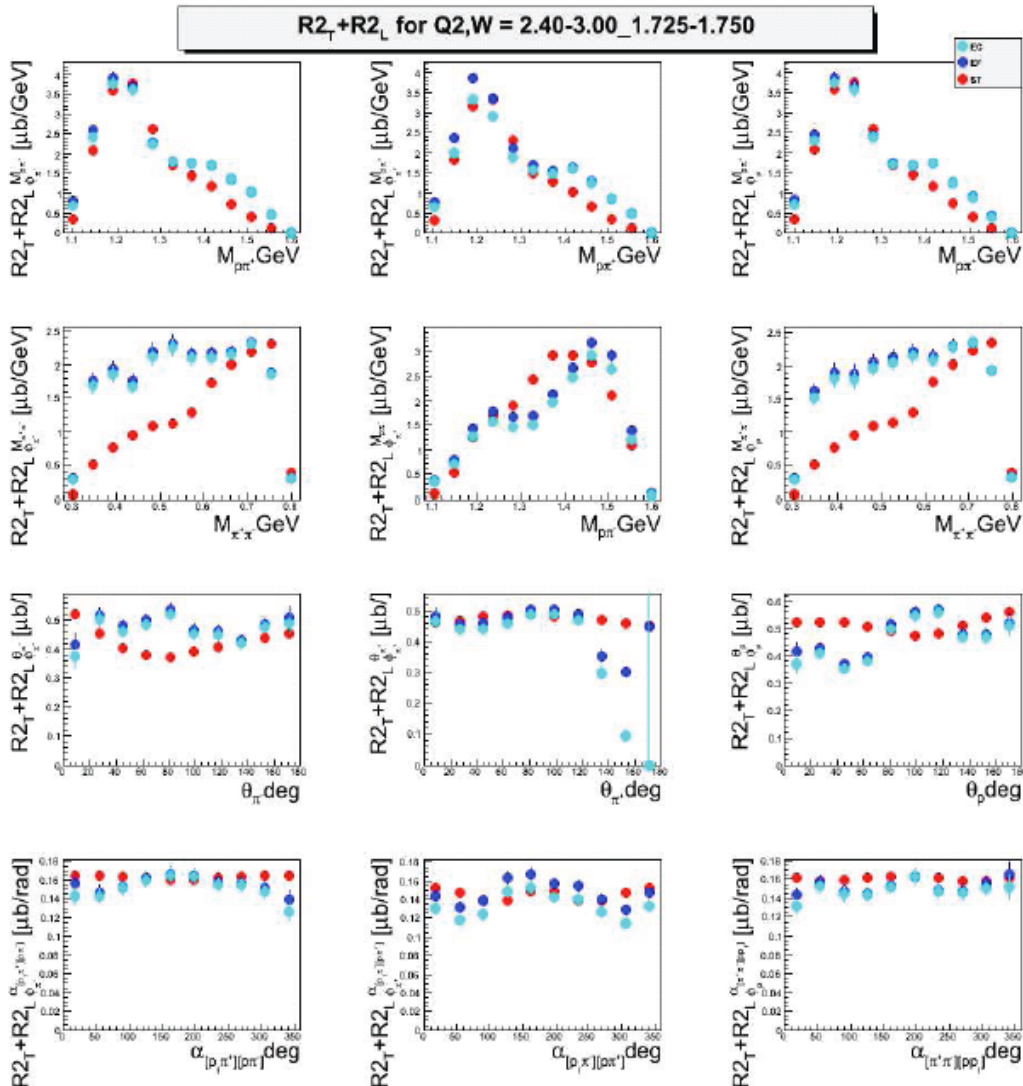


$1.725 \text{ GeV} < W < 1.75 \text{ GeV}$  and  $3 \text{ GeV}^2 < Q^2 < 3.5 \text{ GeV}^2$

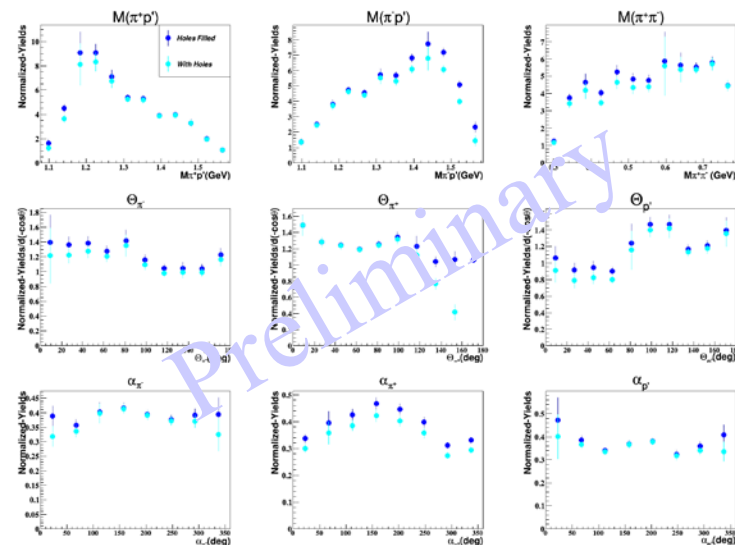
# $\phi$ -dependent $N\pi\pi$ Single-Differential Cross Sections

$Q^2, W$  bin =  $[2.4, 3.0)\text{GeV}^2, [1.725, 1.750)\text{GeV}$

Arjun Trivedi  
Evgeny Isupov



Krishna Neupane  
CLAS12



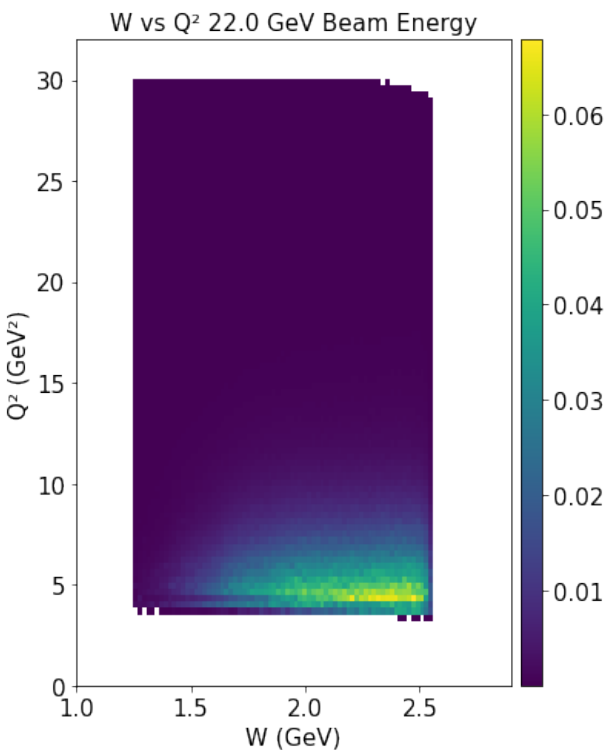
$$\left(\frac{d^2\sigma}{dX_{ij}d\phi_i}\right) = \underline{R2_T X_{ij}} + \underline{R2_L X_{ij}} + R2_{LT}^{c, X_{ij}} \cos \phi_i + R2_{TT}^{c, X_{ij}} \cos 2\phi_i + \delta_{X_{ij}\alpha_i} (R2_{LT}^{s, \alpha_i} \sin \phi_i + R2_{TT}^{s, \alpha_i} \sin 2\phi_i)$$

# CLAS22

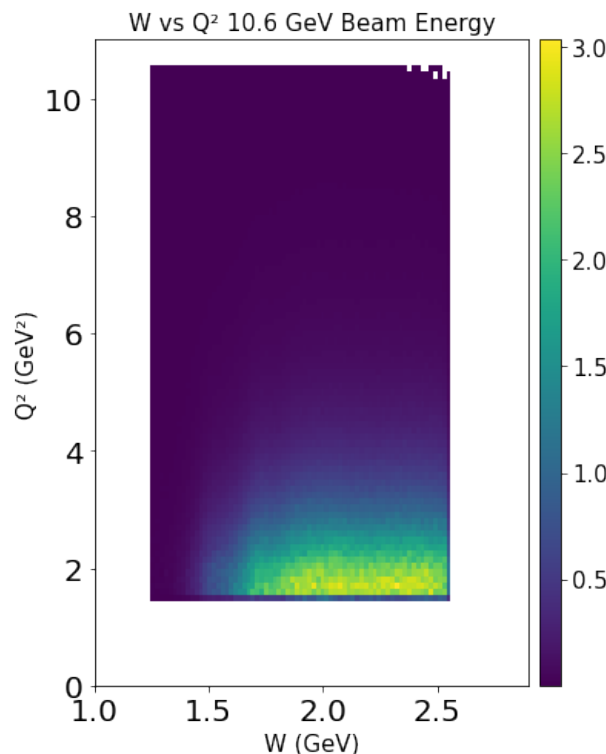
# Achievable (W,Q2) Coverage at 22 GeV

Krishna Neupane

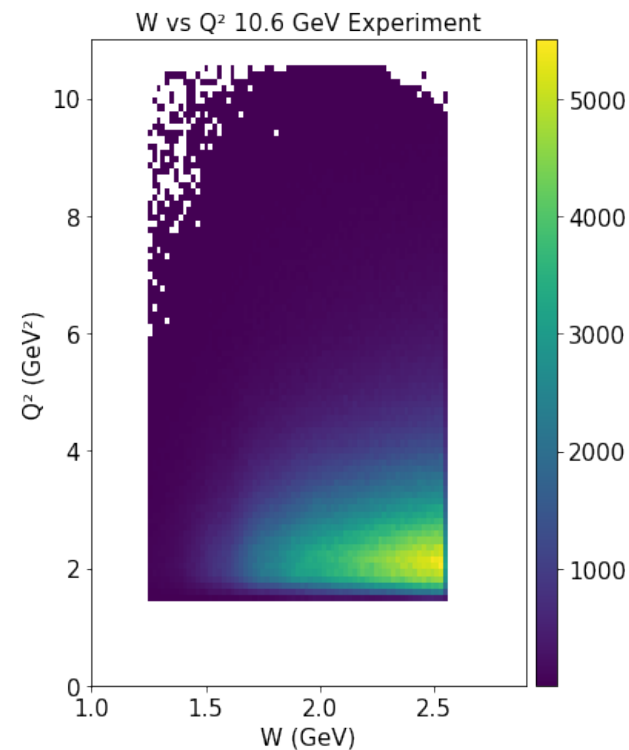
Simulated Reconstructed



Simulated Reconstructed



Measured Reconstructed



HSG is currently simulating:

- ✓  $p\pi^0, n\pi^+$  Maksim Davydov
- ✓ KY Dan Carman
- ✓  $p\pi^+\pi^-$  Krishna Neupane

- Comparison to RGA Fall 2018
- RGA inbending simulation
- Fully exclusive  $p\pi^+\pi^-$

# TWOPEG Formfactor Extrapolation to 30 GeV<sup>2</sup>

Iuliia Skorodumina

$$\frac{d^5\sigma}{d^5\tau}(Q^2) = \frac{d^5\sigma}{d^5\tau}(0.65 \text{ GeV}^2) * \frac{F^2(Q^2)}{F^2(0.65 \text{ GeV}^2)} \quad \text{with } F(Q^2) = \frac{1}{\left(1 + \frac{Q^2}{0.7 \text{ GeV}^2}\right)}$$

point like

monopole

dipole

$$F(Q^2) = 1$$

$$F(Q^2) = \left(1 + \frac{Q^2}{0.7 \text{ GeV}^2}\right)^{-1}$$

$$F(Q^2) = \left(1 + \frac{Q^2}{0.7 \text{ GeV}^2}\right)^{-2}$$

DIS

background

resonance excitation



inclusive, semi-inclusive, exclusive:

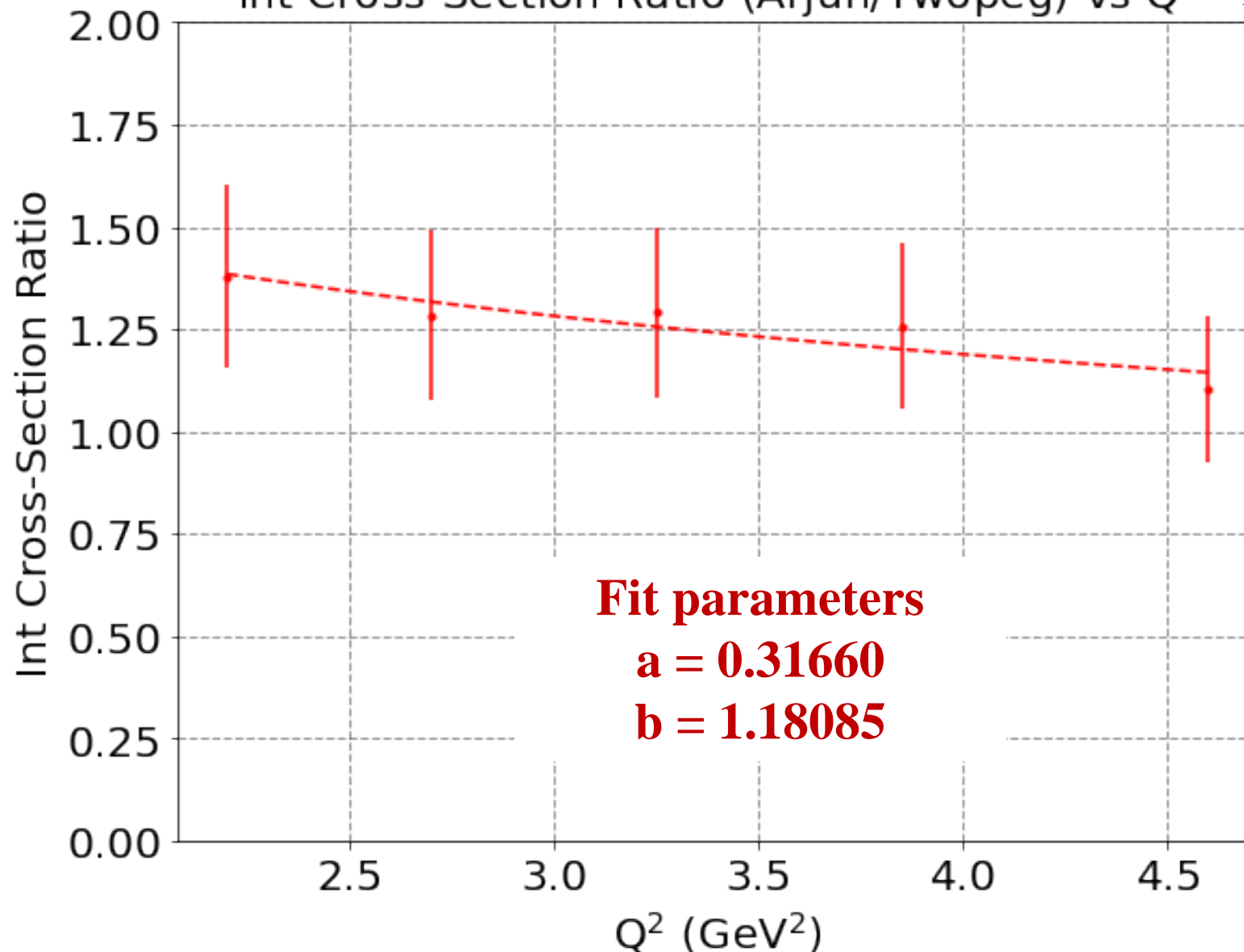
each channel has a different Q<sup>2</sup> dependence



$$\frac{d^5\sigma}{d^5\tau}(Q^2) = \frac{d^5\sigma}{d^5\tau}(0.65 \text{ GeV}^2) * \frac{F^2(Q^2)}{F^2(0.65 \text{ GeV}^2)} * \frac{(F^2(Q^2))^a}{(F^2(0.65 \text{ GeV}^2))^b}$$

# Formfactor Extrapolation to 30 GeV<sup>2</sup>

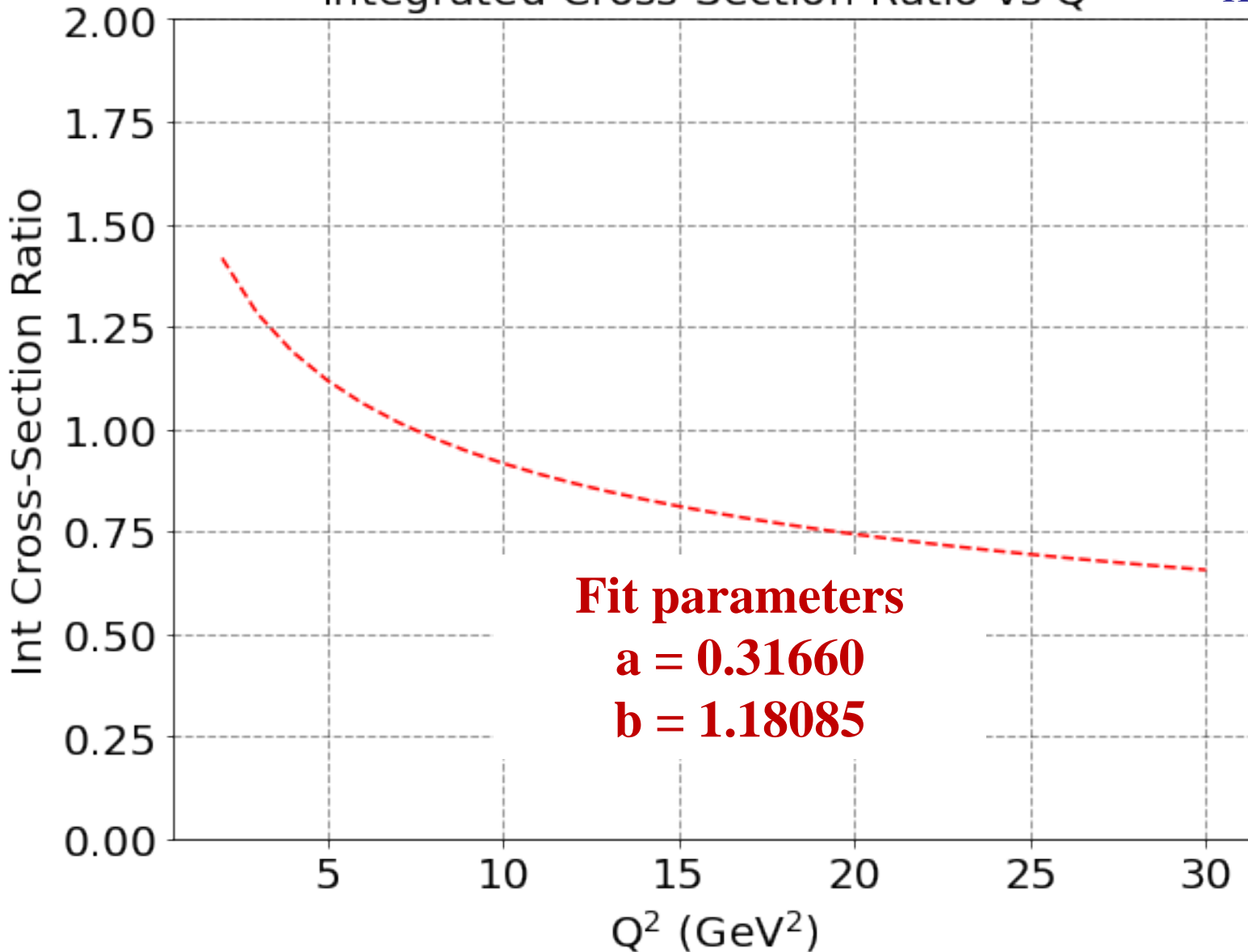
Int Cross-Section Ratio (Arjun/Twopeg) vs Q<sup>2</sup> Krishna Neupane



# Formfactor Extrapolation to 30 GeV<sup>2</sup>

Integrated Cross-Section Ratio vs Q<sup>2</sup>

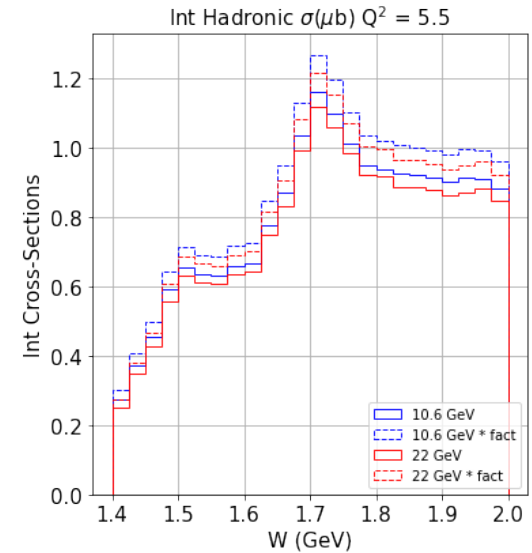
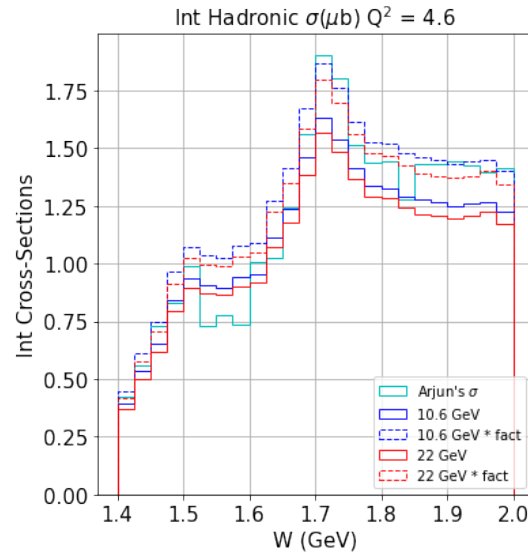
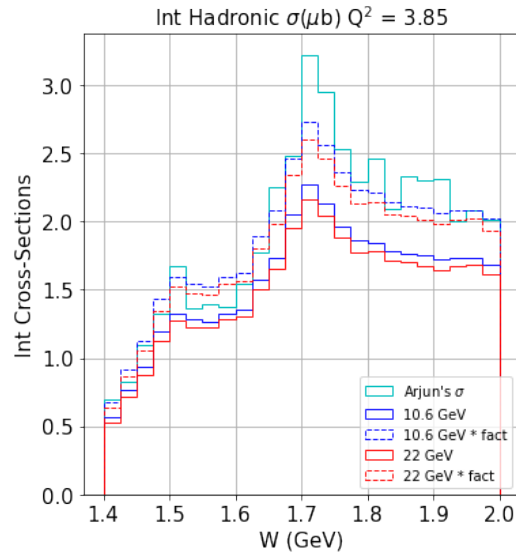
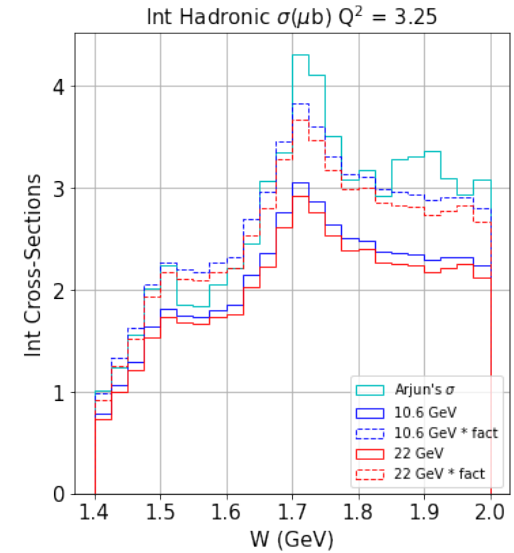
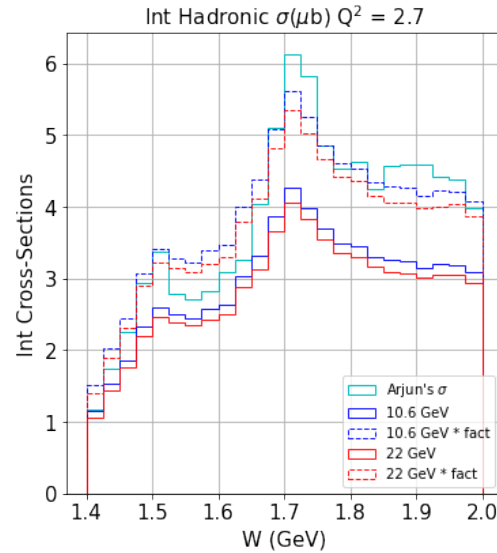
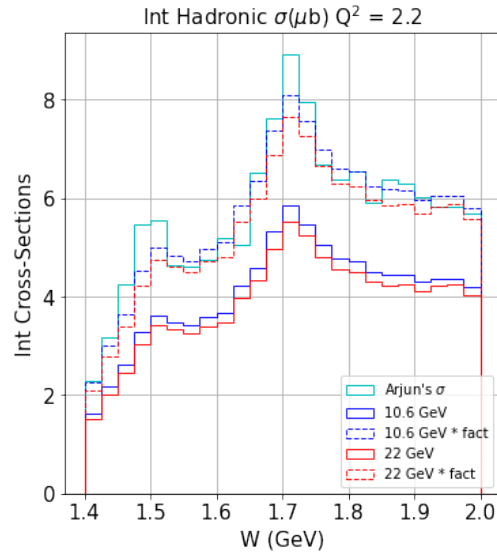
Krishna Neupane





# Formfactor Extrapolation to 30 GeV<sup>2</sup>

Krishna Neupane



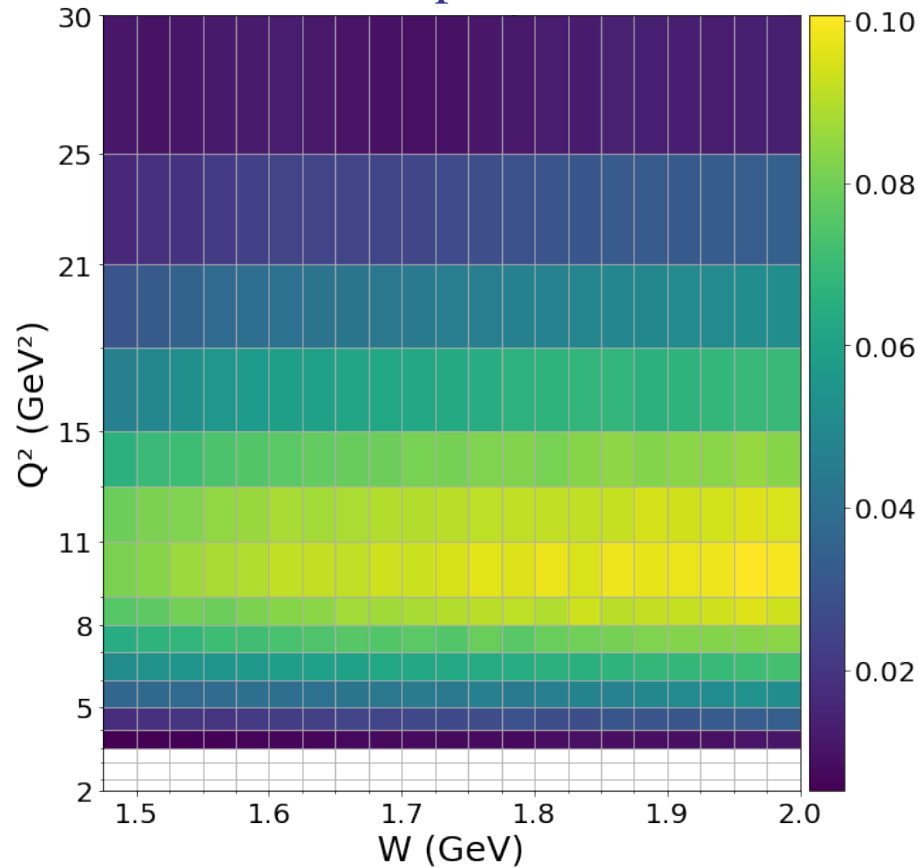
# Acceptance for Exclusive $p\pi^+\pi^-$ Final State

Alexis Osmond & Krishna Neupane

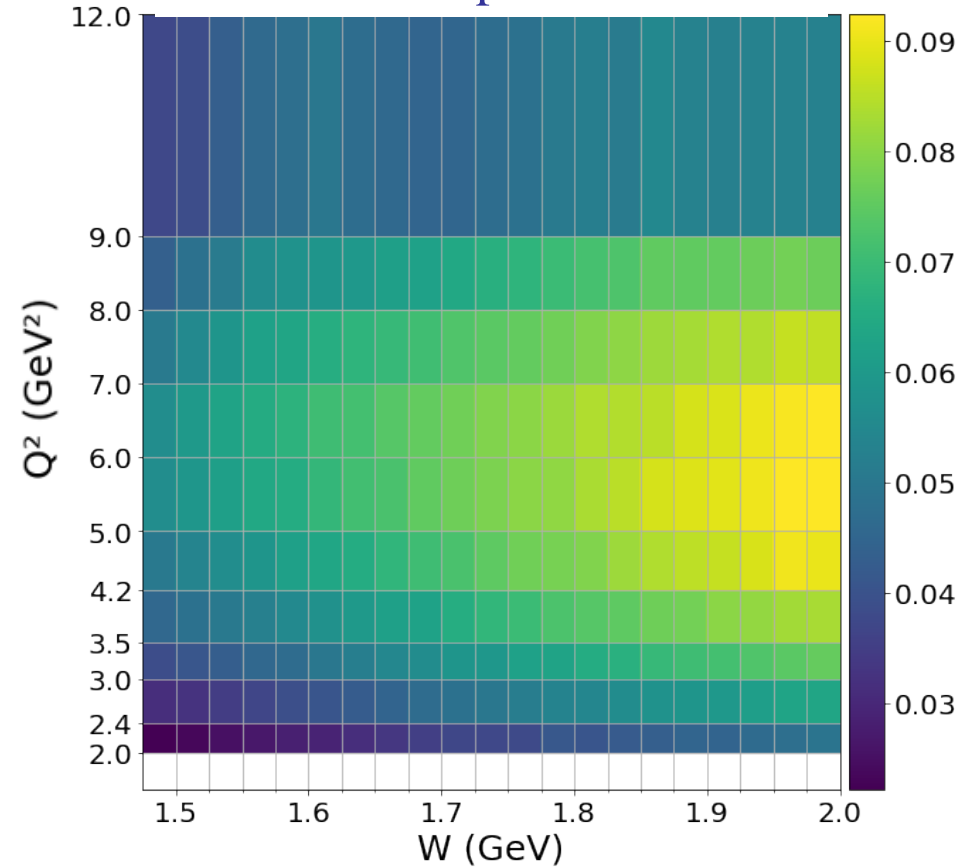
Simulated at 22 GeV Beam Energy

Simulated at 10.6 GeV Beam Energy

Acceptance



Acceptance

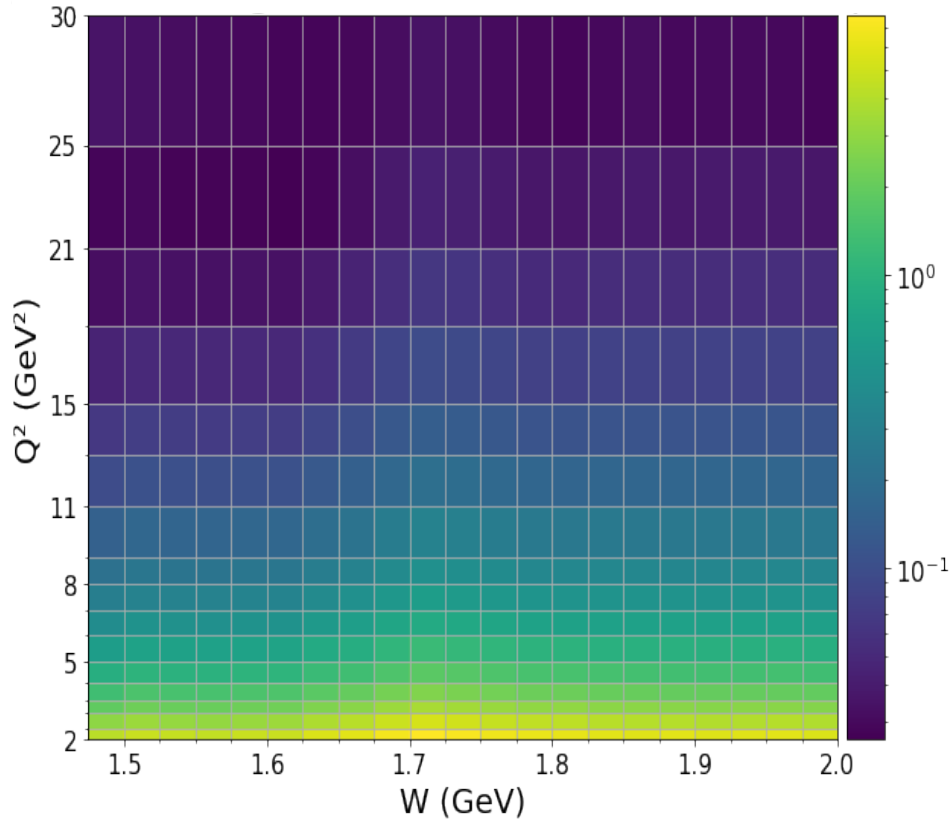


# Hadronic Cross Section for Exclusive $p\pi^+\pi^-$ Final State

Alexis Osmond & Krishna Neupane

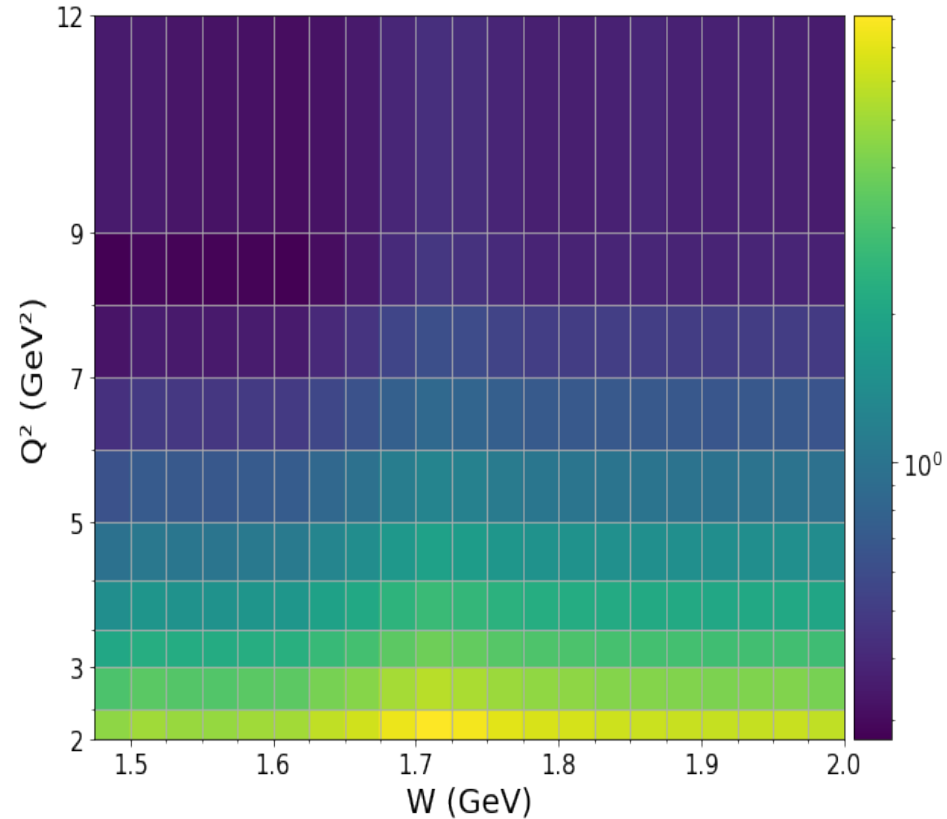
Simulated at 22 GeV Beam Energy

Integrated Hadronic Cross Section ( $\mu\text{b}$ )



Simulated at 10.6 GeV Beam Energy

Integrated Hadronic Cross Section ( $\mu\text{b}$ )



# Integrated Luminosity Needs for Exclusive $p\pi^+\pi^-$

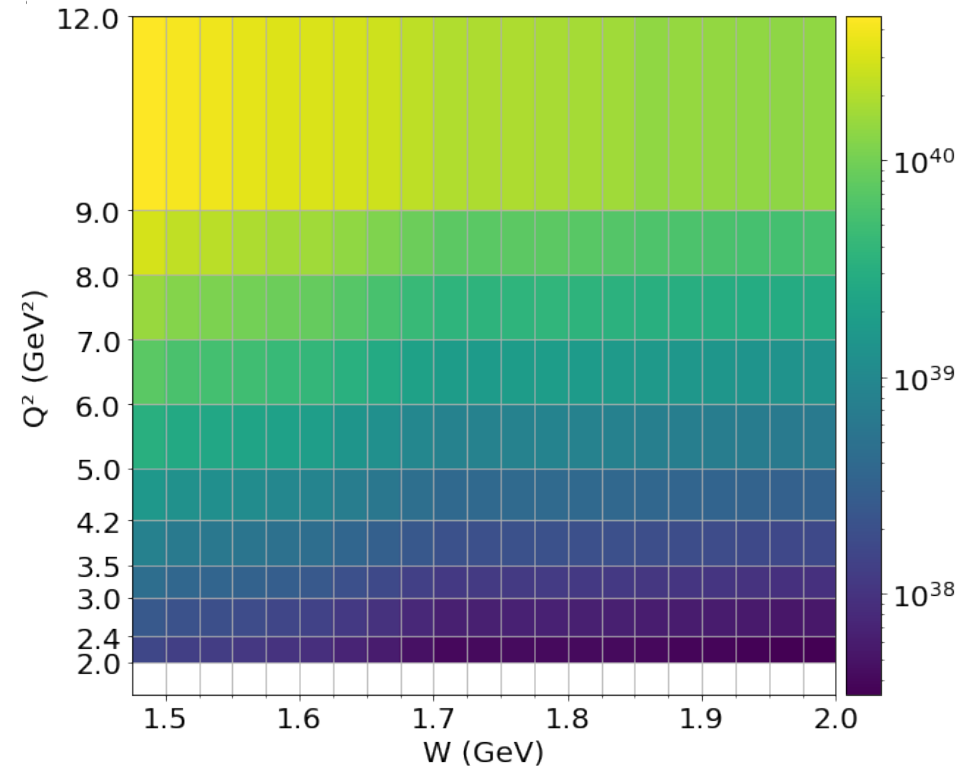
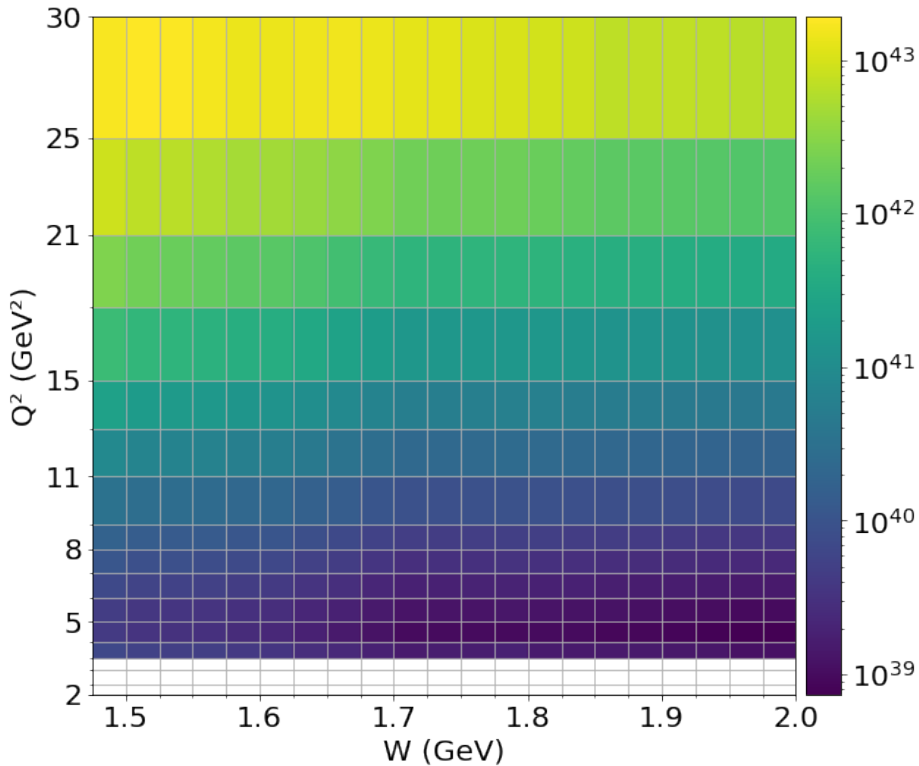
Alexis Osmond & Krishna Neupane

Simulated at 22 GeV Beam Energy

Simulated at 10.6 GeV Beam Energy

Needed Integrated Luminosity ( $\text{cm}^{-2}$ )

Needed Integrated Luminosity ( $\text{cm}^{-2}$ )



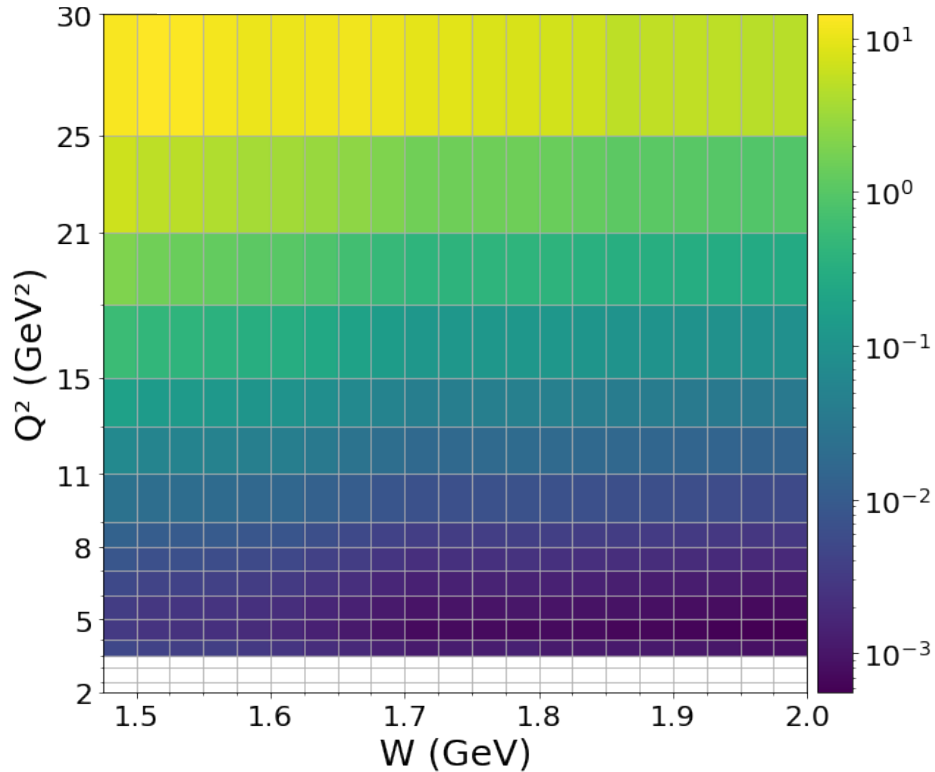
# Integrated Charge Needs for Exclusive $p\pi^+\pi^-$

Alexis Osmond & Krishna Neupane

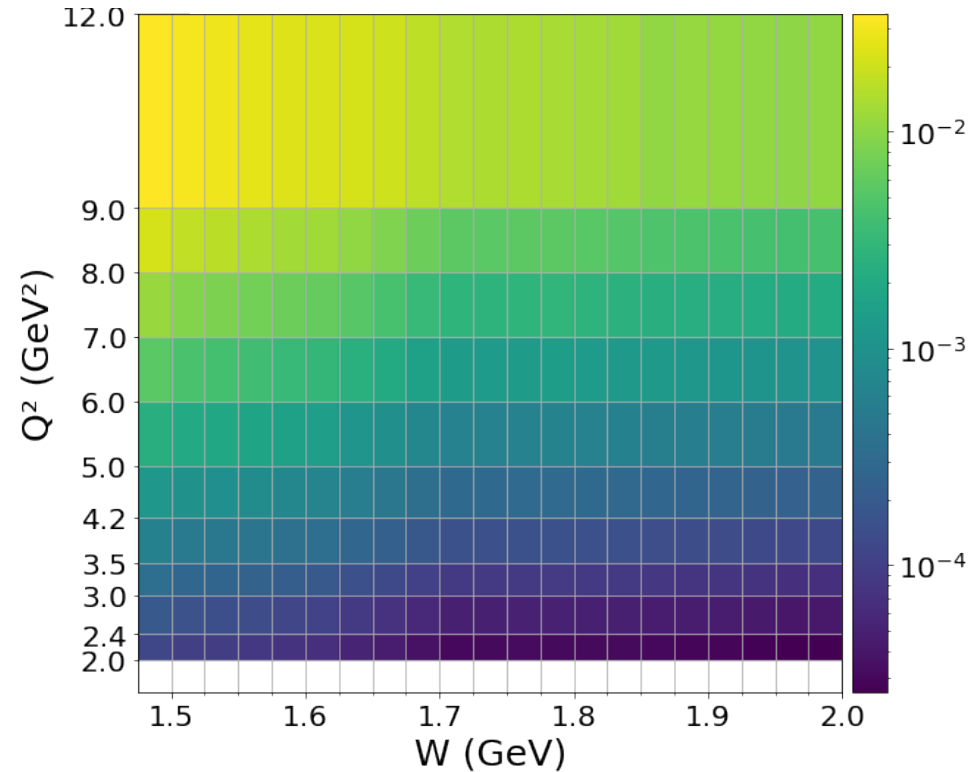
Simulated at 22 GeV Beam Energy

Simulated at 10.6 GeV Beam Energy

Needed Integrated Charge (C)



Needed Integrated Charge (C)



# Beam Time Needs for Exclusive $p\pi^+\pi^-$

Alexis Osmond & Krishna Neupane

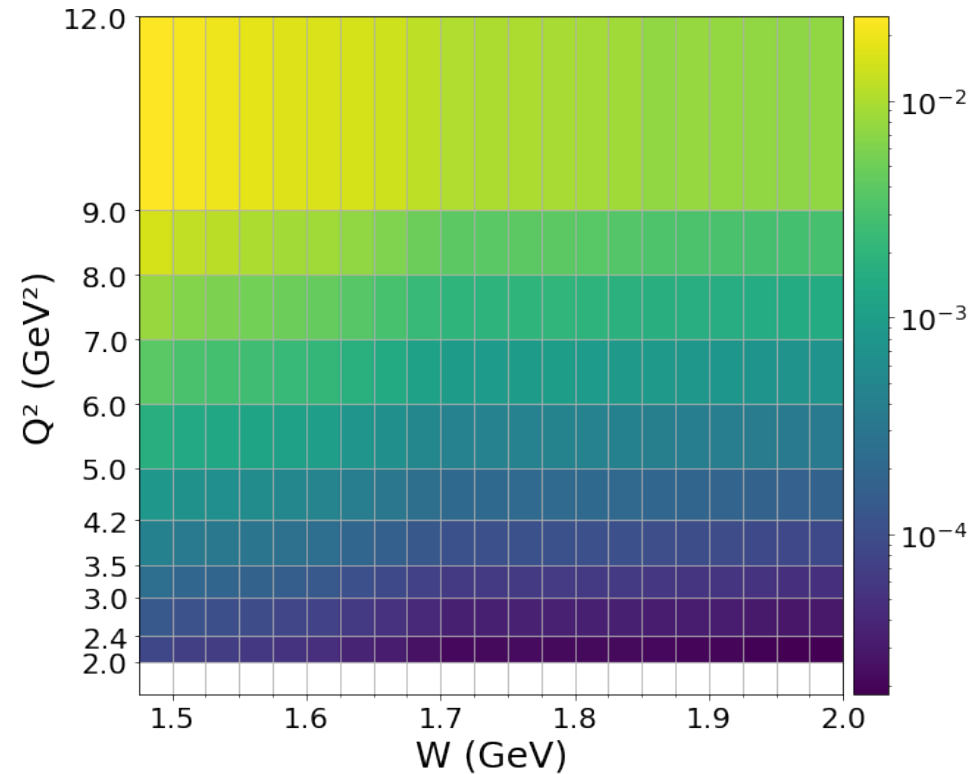
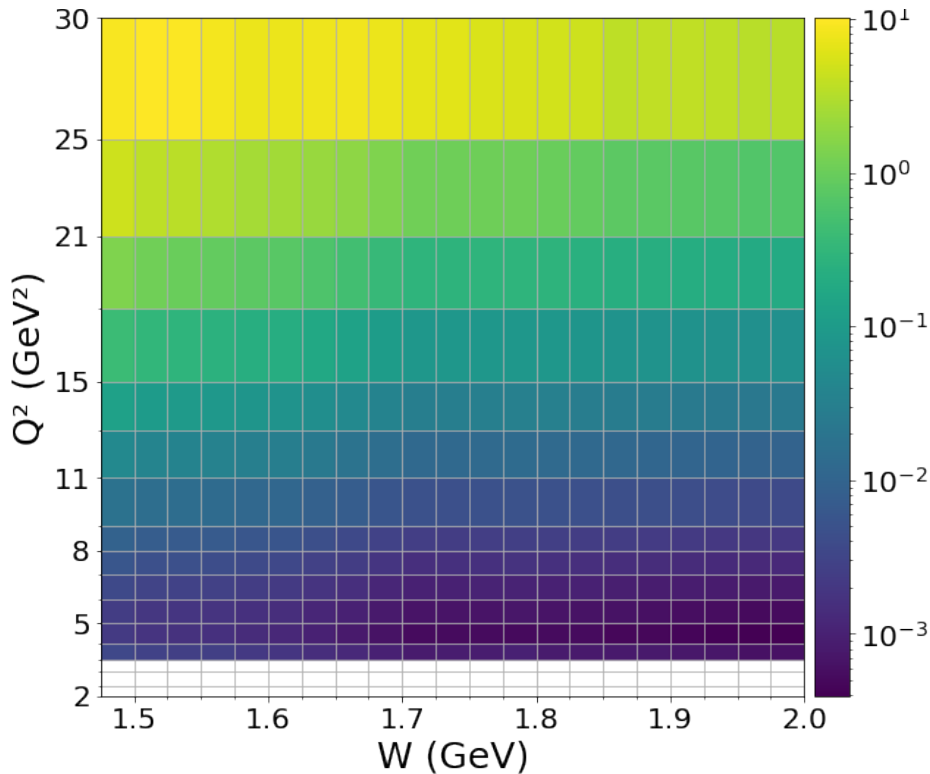
Based on RGA Fall 2018 Luminosity of  $5.96 \cdot 10^{34} \text{ cm}^{-2} \text{ s}^{-1}$  at 45 nA and 5 cm LH<sub>2</sub>

Simulated at 22 GeV Beam Energy

Simulated at 10.6 GeV Beam Energy

Needed Years at  $5.96 \cdot 10^{34} \text{ (cm}^{-2} \text{ s}^{-1})$

Needed Years at  $5.96 \cdot 10^{34} \text{ (cm}^{-2} \text{ s}^{-1})$



Implementing all analysis cuts (3/2), Golden Run Selection (3), PAC Days (2)

➔ 8 (16) years at  $5.96 \cdot 10^{34} \text{ cm}^{-2} \text{ s}^{-1}$  or 11 (22) month at  $5 \cdot 10^{35} \text{ cm}^{-2} \text{ s}^{-1}$

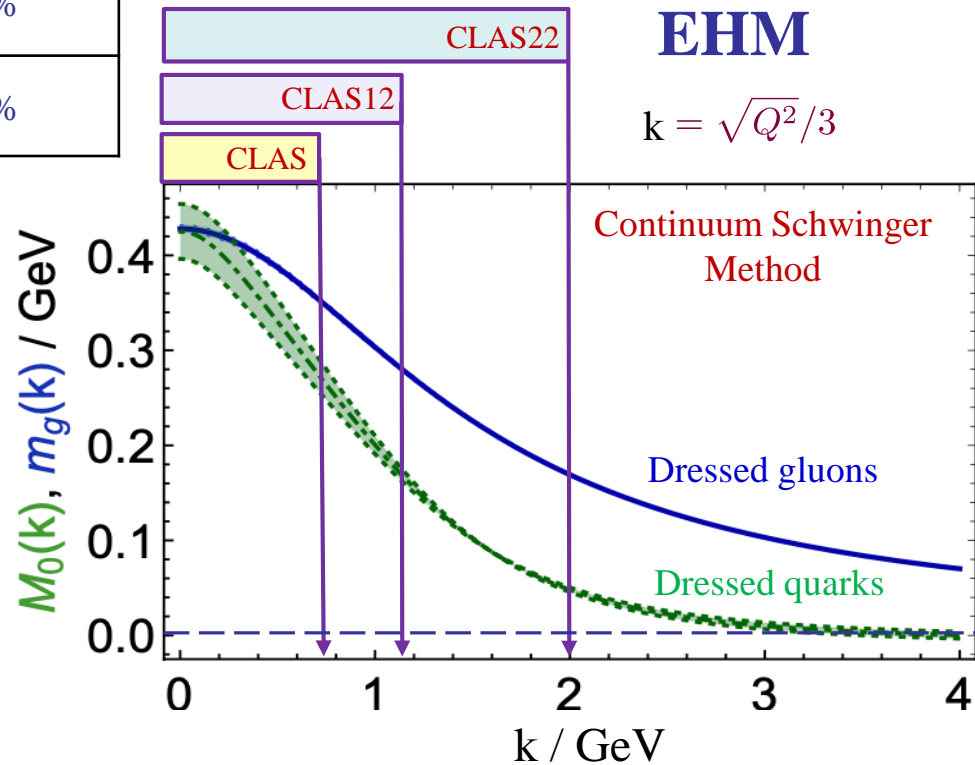
# Hadron Structure Needs for CLAS22

|        | $Q^2$ -coverage of electrocouplings | Range of quark momenta $k$ | Fraction of dressed quark mass at $k < k_{\max}$ |
|--------|-------------------------------------|----------------------------|--------------------------------------------------|
| CLAS   | $< 5 \text{ GeV}^2$                 | $< 0.8 \text{ GeV}$        | 30%                                              |
| CLAS12 | $< 12 \text{ GeV}^2$                | $< 1.2 \text{ GeV}$        | 50%                                              |
| CLAS22 | $< 35 \text{ GeV}^2$                | $< 2.0 \text{ GeV}$        | 90%                                              |

- Beam energy 22 GeV
- Nearly  $4\pi$  acceptance

Increasing knowledge on running dressed quark mass from the results on  $\gamma_p N^*$  electrocouplings.

Measured  $\gamma_p N^*$  electrocouplings of most prominent  $N^*$  states of different structure will provide sound evidence for understanding how the dominant part of the hadron mass and the  $N^*$  structure itself emerge from QCD and will make CEBAF@22 GeV the ultimate QCD-facility at the luminosity frontier.



Luminosity “frontier” is the *unique* advantage of JLab.

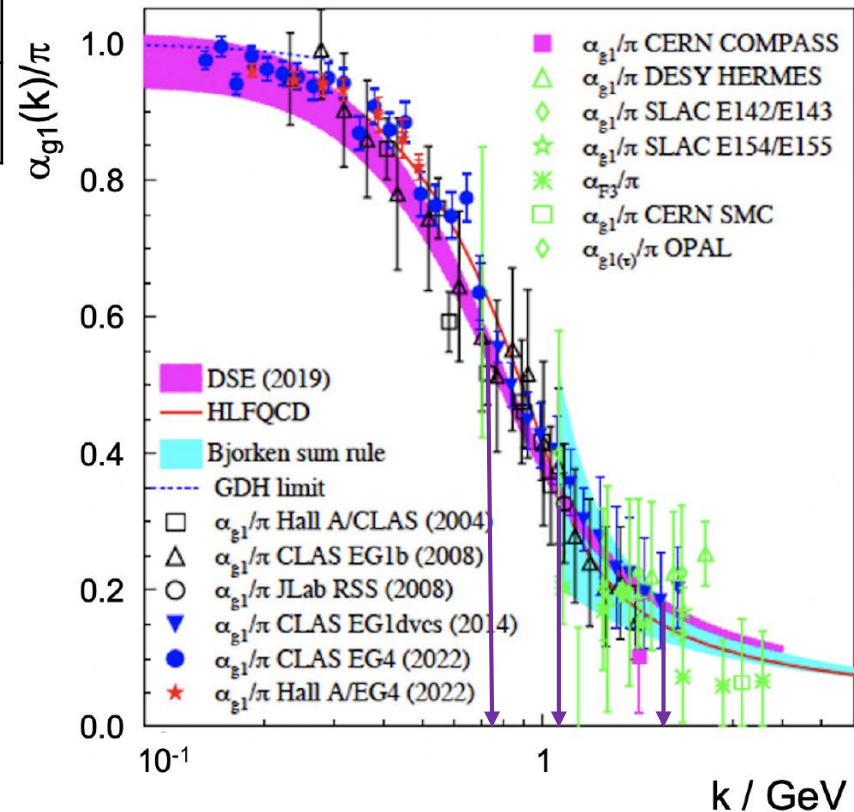
# Hadron Structure Needs for CLAS22

|        | $Q^2$ -coverage of electrocouplings | Range of quark momenta $k$ | Fraction of dressed quark mass at $k < k_{\max}$ |
|--------|-------------------------------------|----------------------------|--------------------------------------------------|
| CLAS   | $< 5 \text{ GeV}^2$                 | $< 0.8 \text{ GeV}$        | 30%                                              |
| CLAS12 | $< 12 \text{ GeV}^2$                | $< 1.2 \text{ GeV}$        | 50%                                              |
| CLAS22 | $< 35 \text{ GeV}^2$                | $< 2.0 \text{ GeV}$        | 90%                                              |

- Beam energy 22 GeV
- Nearly  $4\pi$  acceptance

Increasing knowledge on running dressed quark mass from the results on  $\gamma_{\nu}pN^*$  electrocouplings.

Measured  $\gamma_{\nu}pN^*$  electrocouplings of most prominent  $N^*$  states of different structure will provide sound evidence for **understanding how the dominant part of the hadron mass and the  $N^*$  structure itself emerge from QCD** and will make CEBAF@22 GeV the ultimate QCD-facility at the luminosity frontier.



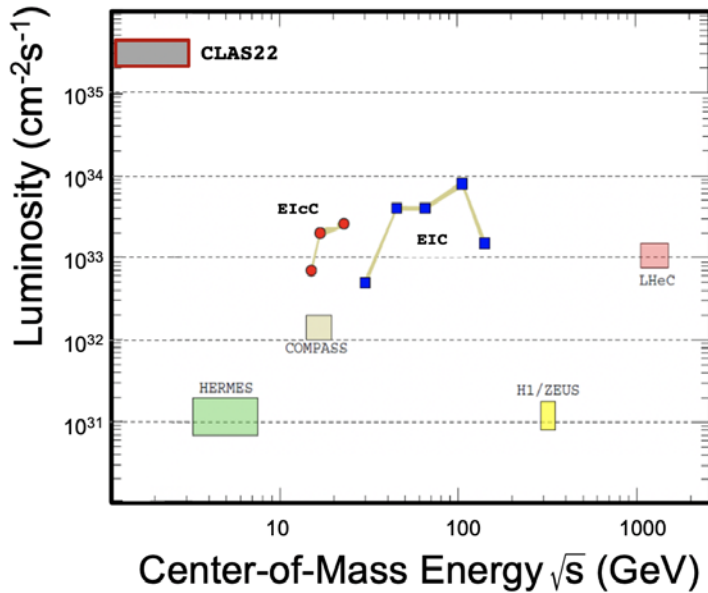
Luminosity “frontier” is the *unique* advantage of JLab.



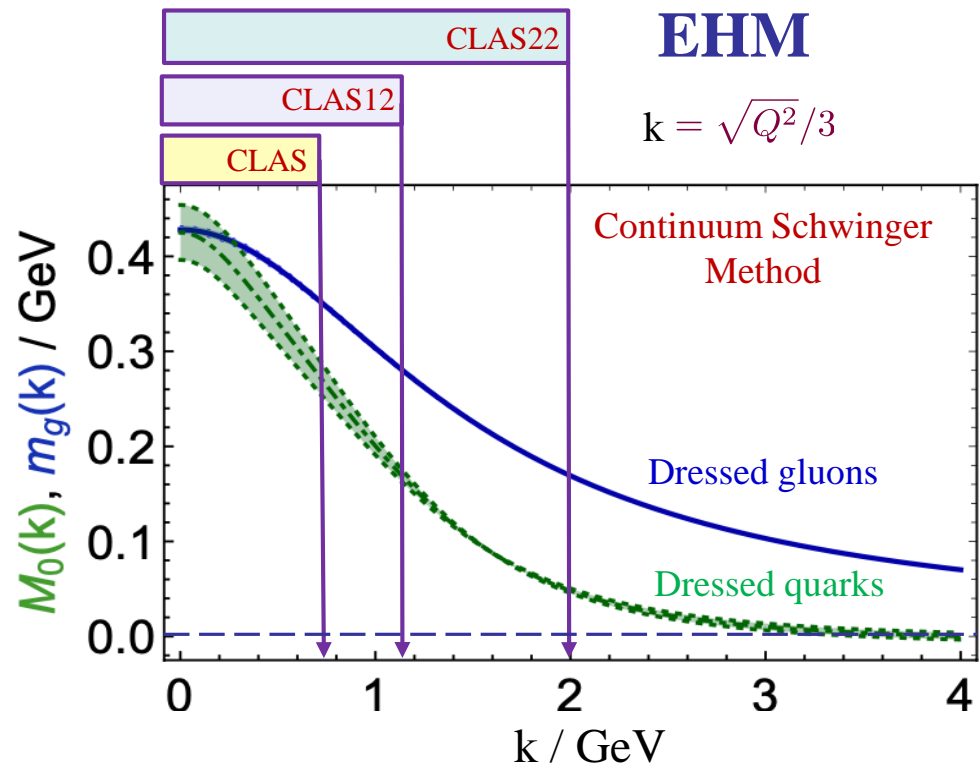
# Hadron Structure Needs for CLAS22

- Beam energy 22 GeV
- Nearly  $4\pi$  acceptance

- High luminosity detector
- High momentum resolution
- Studies of exclusive reactions



Both EIC and EICc would need much higher luminosity to carry out this program.

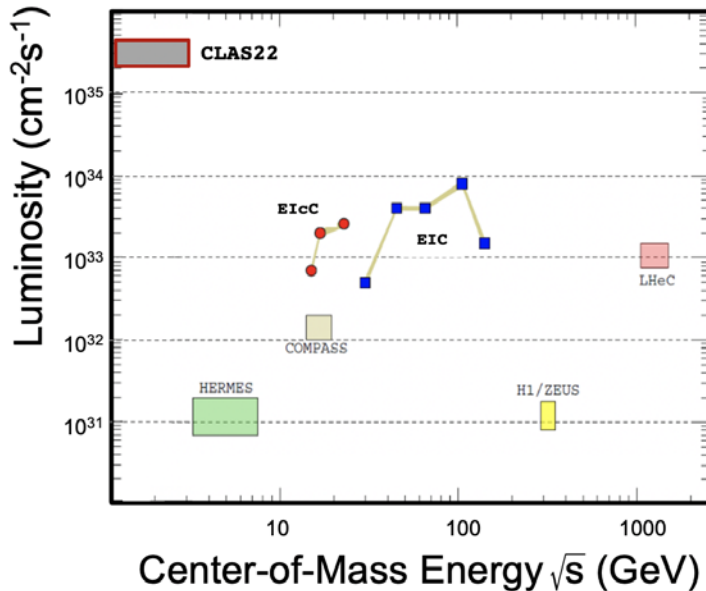


Luminosity “frontier” is the *unique* advantage of JLab.

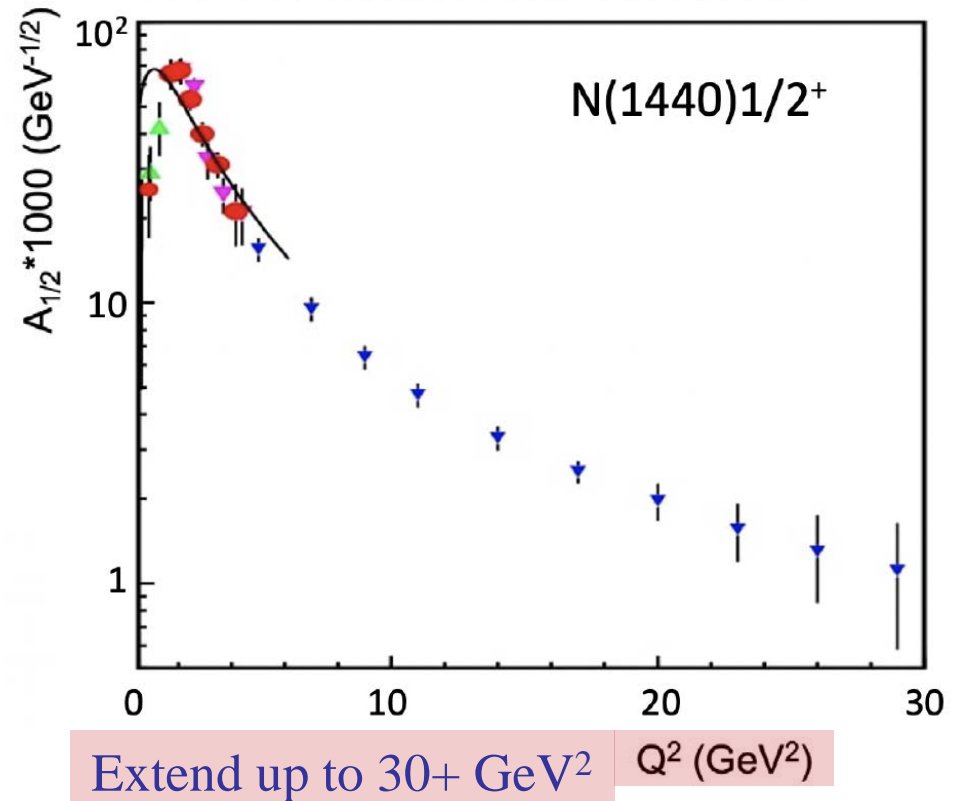
# Hadron Structure Needs for CLAS22

- Beam energy 22 GeV
- Nearly  $4\pi$  acceptance

- High luminosity detector
- High momentum resolution
- Studies of exclusive reactions



Both EIC and EICc would need much higher luminosity to carry out this program.



Luminosity “frontier” is the *unique* advantage of JLab.

# JLab @ 22 GeV and EHM

Strong Interaction Physics at the Luminosity Frontier  
with 22 GeV Electrons at Jefferson Lab

e-Print: 2306.09360  
accepted in EPJA

arXiv:2306.09360v2 [nucl-ex] 24 Aug 2023

A. Accardi<sup>1</sup>, P. Achenbach<sup>2</sup>, D. Adhikari<sup>3</sup>, A. Afanasev<sup>4</sup>, C.S. Akondi<sup>5</sup>, N. Akopov<sup>6</sup>,  
M. Albaladejo<sup>7</sup>, H. Albataineh<sup>8</sup>, M. Albrecht<sup>2</sup>, B. Almeida-Zamora<sup>9</sup>, M. Amarian<sup>10</sup>,  
D. Androić<sup>11</sup>, W. Armstrong<sup>12</sup>, D.S. Armstrong<sup>13</sup>, M. Arratia<sup>14</sup>, J. Arrington<sup>15</sup>,  
A. Asaturyan<sup>16</sup>, A. Austregesilo<sup>2</sup>, H. Avagyan<sup>2,\*</sup>, T. Averett<sup>13</sup>, C. Ayerbe Gayoso<sup>13</sup>,  
A. Bacchetta<sup>17</sup>, A.B. Balantekin<sup>18</sup>, N. Baltzell<sup>2</sup>, L. Barion<sup>19</sup>, P. C. Barry<sup>2</sup>, A. Bashir<sup>20,2</sup>,  
M. Battaglieri<sup>21</sup>, V. Bellini<sup>22</sup>, I. Belov<sup>21</sup>, O. Benhar<sup>23</sup>, B. Benkel<sup>24</sup>, F. Benmokhtar<sup>25</sup>,  
W. Bentz<sup>26</sup>, V. Bertone<sup>27</sup>, H. Bhatt<sup>28</sup>, A. Bianconi<sup>29</sup>, L. Bibrzycki<sup>30</sup>, R. Bijker<sup>31</sup>,  
D. Binosi<sup>32</sup>, D. Biswas<sup>3</sup>, M. Boër<sup>3</sup>, W. Boeglin<sup>33</sup>, S.A. Bogacz<sup>2,\*</sup>, M. Boggione<sup>34</sup>,  
M. Bondi<sup>22</sup>, E.E. Boos<sup>35</sup>, P. Bosted<sup>13</sup>, G. Bozzi<sup>36</sup>, E.J. Brash<sup>37</sup>, R. A. Briceño<sup>38</sup>,  
P.D. Brindza<sup>10</sup>, W.J. Briscoe<sup>4</sup>, S.J. Brodsky<sup>39</sup>, W.K. Brooks<sup>40,41,42</sup>, V.D. Burkert<sup>2</sup>,  
A. Camsonne<sup>2</sup>, T. Cao<sup>2</sup>, L.S. Cardman<sup>2</sup>, D.S. Carman<sup>2</sup>, M. Carpinelli<sup>43</sup>, G.D. Cates<sup>44</sup>,  
J. Caylor<sup>2</sup>, A. Celentano<sup>21</sup>, F.G. Celiberto<sup>45</sup>, M. Cerutti<sup>17</sup>, Lei Chang<sup>46</sup>, P. Chatagnon<sup>2</sup>,  
C. Chen<sup>47,48</sup>, J.P. Chen<sup>2,\*</sup>, T. Chen<sup>33</sup>, A. Chini<sup>49</sup>, J. Chino<sup>2</sup>, F. Chiodini<sup>2</sup>, F. Chiodini<sup>2</sup>,  
E. Cisba<sup>2</sup>, P.L. Cioara<sup>2</sup>, C. Cottle<sup>2</sup>, M. Döring<sup>2</sup>, Napoli<sup>22</sup>, P. Di Nevo<sup>2</sup>, S. Dörmann<sup>2</sup>, G. Ecker<sup>2</sup>,  
A. Emmert<sup>2</sup>, S. Fegan<sup>7</sup>, C.S. Fischer<sup>2</sup>, L. Gamberger<sup>2</sup>, K. Gates<sup>2</sup>,  
G.-P. Gilfoyle<sup>87</sup>, F-X Girod<sup>2</sup>, D. I. Glazier<sup>84</sup>, C. Gleason<sup>88</sup>, S. Godfrey<sup>89</sup>, J.L. Goity<sup>2,1</sup>,  
A.A. Golubenko<sup>35</sup>, S. González-Solís<sup>90</sup>, R.W. Gothe<sup>91,\*</sup>, Y. Gotra<sup>2</sup>, K. Griffioen<sup>13</sup>,  
O. Grocholski<sup>92</sup>, B. Grube<sup>2</sup>, P. Guèye<sup>79</sup>, F.-K. Guo<sup>93,94</sup>, Y. Guo<sup>95</sup>, L. Guo<sup>33</sup>, T. J. Hague<sup>15</sup>,  
N. Hammoud<sup>85</sup>, J.-O. Hansen<sup>2</sup>, M. Hattawy<sup>10</sup>, F. Hauenstein<sup>2</sup>, T. Hayward<sup>62</sup>, D. Heddle<sup>37</sup>,  
N. Heinrich<sup>96</sup>, O. Hen<sup>67</sup>, D.W. Higinbotham<sup>2</sup>, I.M. Higuera-Angulo<sup>97</sup>, A. N. Hiller Blin<sup>98</sup>, ...



\* 16 editors  
444 authors

Strong Interaction Physics at the Luminosity Frontier  
with 22 GeV Electrons at Jefferson Lab

e-Print: 2306.09360  
accepted in EPJA

## 6.5 Bound Three-Quark Structure of Excited Nucleons and Emergence of Hadron Mass

D.S. Carman, R.W. Gothe, V.I. Mokeev, C.D. Roberts

### 6.5.1 The Emergent Hadron Mass Paradigm

The Standard Model of Particle Physics has one well-known mass-generating mechanism for the most elementary constituents of Nature, *viz.* the Higgs boson [295, 296], which is critical to the evolution of the Universe. Yet, alone, the Higgs is responsible for just 1% of the visible mass in the Universe. Visible matter is constituted from nuclei found on Earth and the mass of each such nucleus is largely the sum of the masses of the nucleons they contain. However, only 9 MeV of a nucleon's mass,  $m_N = 940$  MeV, is directly generated by Higgs boson couplings into quantum chromodynamics (QCD). Evidently, as highlighted by Fig. 46, Nature has another, very effective, mass-generating mechanism. Often called emergent hadron mass (EHM) [202, 297–299], it is responsible for 94% of  $m_N$ , with the remaining 5% generated by constructive interference between EHM and the Higgs boson. This makes studies of the structure of ground and excited nucleon states in experiments with electromagnetic probes a most promising avenue to gain insight into the strong interaction dynamics that underlie the emergence of the dominant part of the visible mass in the Universe [105, 202, 300–302].

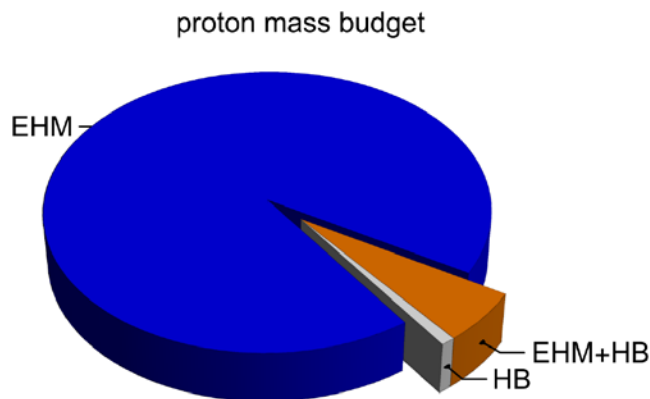




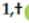

Figure 46: Proton mass budget, drawn using a Poincaré-invariant decomposition: emergent hadron mass (EHM) = 94%; Higgs boson (HB) contribution = 1%; and EHM+HB interference = 5%. (Separation at renormalization scale  $\zeta = 2$  GeV, calculated using information from Refs. [22, 303–305]).

\* 16 editors  
444 authors

arXiv:2306.09360v2 [nucl-ex] 24 Aug 2023

...

## Nucleon Resonance Electroexcitation Amplitudes and Emergent Hadron Mass

Daniel S. Carman <sup>1,†</sup> , Ralf W. Gothe <sup>2,†</sup> , Victor I. Mokeev <sup>1,†</sup> , and Craig D. Roberts <sup>3,4,†</sup> \*

**Abstract:** Understanding the strong interaction dynamics that govern the emergence of hadron mass (EHM) represents a challenging open problem in the Standard Model. In this paper we describe new opportunities for gaining insight into EHM from results on nucleon resonance ( $N^*$ ) electroexcitation amplitudes (*i.e.*  $\gamma_v p N^*$  electrocouplings) in the mass range up to 1.8 GeV for virtual photon four-momentum squared (*i.e.* photon virtualities  $Q^2$ ) up to  $7.5 \text{ GeV}^2$  available from exclusive meson electroproduction data acquired during the 6-GeV era of experiments at Jefferson Laboratory (JLab). These results, combined with achievements in the use of continuum Schwinger function methods (CSMs), offer new opportunities for charting the momentum dependence of the dressed quark mass from results on the  $Q^2$ -evolution of the  $\gamma_v p N^*$  electrocouplings. This mass function is one of the three pillars of EHM and its behavior expresses influences of the other two, *viz.* the running gluon mass and momentum-dependent effective charge. A successful description of the  $\Delta(1232)3/2^+$  and  $N(1440)1/2^+$  electrocouplings has been achieved using CSMs with, in both cases, common momentum-dependent mass functions for the dressed quarks, for the gluons, and the same momentum-dependent strong coupling. The properties of these functions have been inferred from nonperturbative studies of QCD and confirmed, *e.g.*, in the description of nucleon and pion elastic electromagnetic form factors. Parameter-free CSM predictions for the electrocouplings of the  $\Delta(1600)3/2^+$  became available in 2019. The experimental results obtained in the first half of 2022 have confirmed the CSM predictions. We also discuss prospects for these studies during the 12-GeV era at JLab using the CLAS12 detector, with experiments that are currently in progress, and canvass the physics motivation for continued studies in this area with a possible increase of the JLab electron beam energy up to 22 GeV. Such an upgrade would finally enable mapping of the dressed quark mass over the full range of distances (*i.e.* quark momenta) where the dominant part of hadron mass and  $N^*$  structure emerge in the transition from the strongly coupled to perturbative QCD regimes.



Citation: Carman, D.S.; Gothe, R.W.; Mokeev, V.I.; and Roberts, C.D. Nucleon Resonance Electroexcitation and Emergent Hadron Mass. *Particles* 2023, 1, 1–23. <https://doi.org/>

Received: 2023 Jan 09

Accepted:

Published: